FINAL REPORT

PROJECT B-3828
(National Science Foundation Institutional Grant -
1970 - Grant No. GU-3309)

AUTOMATED RADIO FREQUENCY ASSIGNMENT TECHNIQUES FOR TROPOSPHERIC SCATTER COMMUNICATIONS

E. T. Hungerford

June 30, 1971

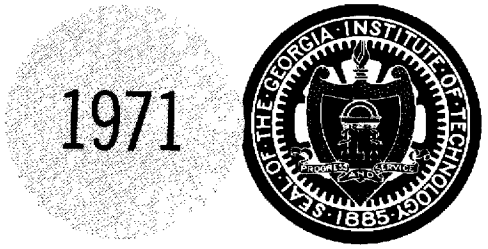

Rich Electronic Computer Center
GEORGIA INSTITUTE OF TECHNOLOGY
Atlanta, Georgia

FINAL REPORT

PROJECT B-3828

(National Science Foundation Institutional Grant - 1970
Grant No. GU-3309)

AUTOMATED RADIO FREQUENCY ASSIGNMENT TECHNIQUES FOR TROPOSPHERIC SCATTER COMMUNICATIONS

E. T. Hungerford

June 30, 1971

Rich Electronic Computer Center
GEORGIA INSTITUTE OF TECHNOLOGY
Atlanta, Georgia

Abstract

This work represents a brief investigation into the characteristics of troposcatter propagation far beyond the horizon. Background discussions are presented on troposcatter path plots as well as spherical diffraction paths. The results of various theories for troposcatter propagation are presented with respect to predictions of received tropo signal levels. The principal parameters which appear to affect received tropo signal levels are identified. Based on both theoretical and empirical relationships, the quantitative effects of the various parameters on received signal levels are discussed and displayed in the form of figures or charts. Empirical relationships are established for the prediction or received tropo signal levels, including signal variations, for any arbitrary tropo path. In general, tropo paths are categorized according to climatic location, which permits a first order prediction of received signal level. Estimated corrections to these signal levels may then be applied according to the existent values of the other principal parameters. Finally, frequency requirements and procedures are discussed for equipments operated in a tropo network. Specific frequency separation requirements are developed as an example for AN/TRC-90B equipment for controlling both cosite and off-site interference in tropo networks. Recommended frequency management and assignment procedures are included.

Table of Contents

List of Figures

A. Background Discussions

1. The troposphere is that portion of the earth's atmosphere which extends from the surface upwards to approximately 12 miles. The upper limit is not well-defined, since atmospheric constituents and characteristics change continuously from the troposphere into the stratosphere. Perhaps a useful height limit for troposcatter communications would be 6 miles (10 km). At this height the three-fold reduction in pressure and density amounts to a significant reduction in the "scattering" medium itself.

2. The index of refraction of the troposphere is one atmospheric parameter which represents a composite measure of several of the more important characteristics of the troposphere. At radio frequencies, the refractive index n may be expressed as[1]

$$n = 1 + \left[\frac{103.49}{T}(p-e) + 86.26\,\frac{e}{T}\left(1 + \frac{5748}{T}\right)\right] \times 10^{-6}, \qquad 1$$

where T is the temperature in degrees Kelvin, and p and e are the pressure and vapor pressure, respectively, measured in millimeters of mercury. A more convenient term called the coindex is often utilized, where

$$N\ (\text{coindex}) = (n-1) \times 10^{6}. \qquad 2$$

3. In general, the mean value of the refractive index decreases with height in an exponential manner. For a standard atmosphere, N has been defined as[2]

$$N = 289 \times e^{-0.136h}, \qquad 3$$

where N is the coindex, and h is the height measured in kilometers. At heights

less than about 5 km, a linear approximation is often utilized as

$$N = 289 - 39h \qquad 4$$

where the value of 289 N units is representative of the surface coindex for a standard atmosphere, and where h is the height, measured in kilometers. The value of -39 in equation 4 has been defined as the standard gradient, g. Dependent on geographical location, g may vary typically between -10 and -80 N units/km for the lower heights ($\leq$ 5 km).

4. The mean decrease of the refractive index with height will cause radio waves propagating in the troposphere to be refracted (bent back) toward the earth's surface. The degree of bending decreases with increasing frequency. However, for the frequencies of interest in the communication bands, the convex propagation paths can be represented adequately as ray paths (straight lines), if an appropriately enlarged (fictitious) earth radius is utilized. A sketch of the development is given as follows.

a. If the troposphere is assumed to be homogeneous ($\Delta n = 0$), propagation paths are straight lines. This is depicted in Figure 1 for a smooth real earth of radius r. A transmitter is assumed located at point A on the surface; the tangent to the surface at point A intercepts the vertical axis at y distance from the surface (or at y + r distance from the earth's center). A transmitter elevation angle, α_o, is indicated for the propagation path from point A to point B, intercepting the vertical axis at a height h above the earth's surface. At point B, the propagation path angle with the horizontal is indicated as α. From construction, $\alpha = \theta + \alpha_o$. Therefore,

$$\cos\alpha = \cos(\theta + \alpha_o) = \cos\theta\cos\alpha_o - \sin\theta\sin\alpha_o. \qquad 5$$

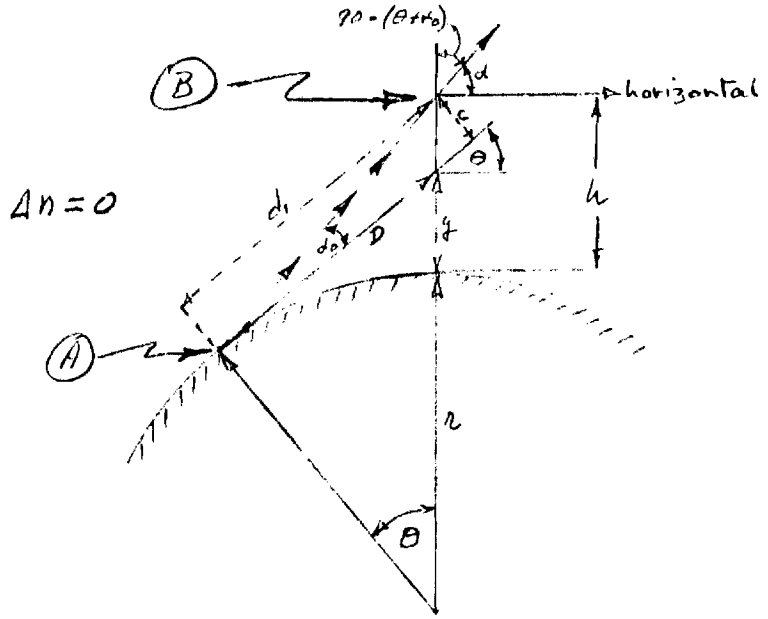

$\alpha = \theta + \alpha_0$

$c = (h-y)\cos\theta$

$d_1 = (n+h)\sin\theta$

$y = \frac{r(1-\cos\theta)}{\cos\theta}$

FIGURE 1

Rectilinear Paths

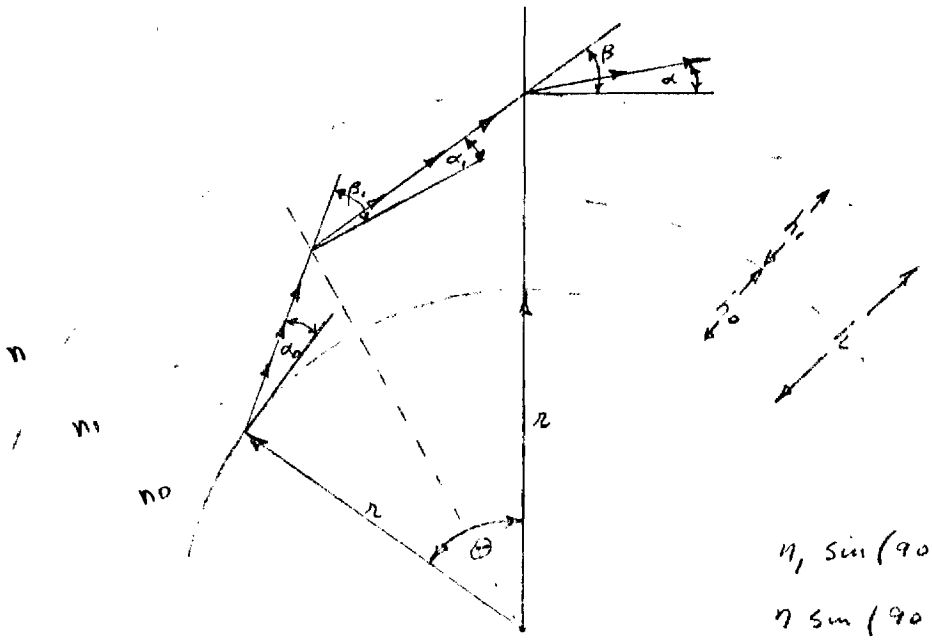

$\eta_1 \sin(90-\alpha_1) = \eta_0 \sin(90-\beta_1)$

$\eta \sin(90-\alpha) = \eta_1 \sin(90-\beta)$

FIGURE 2

Stratified Medium, Rectilinear Paths

Also from construction, we have

$$\sin \alpha_o = \left[\frac{h \cos\theta - r(1 - \cos \alpha)}{(r + h) \sin \theta} \right] \cos \alpha_o \quad . \qquad 6$$

After substitution of equation 6 into equation 5, we obtain

$$\cos \alpha_o = \left(1 + \frac{h}{r} \right) \cos \alpha \quad . \qquad 7$$

Equation 7 establishes the relationship between the transmitter elevation angle, α_o, the earth's radius, r, and the resultant path angle, α, with respect to the horizontal at some height h above the earth's surface. The form of equation 7 is important in that it represents rectilinear propagation in a homogeneous troposphere.

b. In Figure 2, the troposphere is assumed to be stratified into homogeneous layers as indicated. Therefore, within each layer (n_o, n_1, and n) the propagation path can be represented as a straight line (ray path). For the layer next to the earth's surface, utilizing equation 7 above, we have

$$r \cos \alpha_o = (r + h_o) \cos \beta_1 \quad . \qquad 8$$

From Huygens' principle, we have

$$n_1 \sin (90° - \alpha_1) = n_o \sin (90° - \beta_1), \qquad 9$$

or

$$\cos \beta_1 = \frac{n_1}{n_o} \cos \alpha_1 \quad .$$

Substitution of equation 9 into equation 8 yields

$$r \cos_o = \left(r + h_o\right) \frac{n_1}{n_o} \cos \alpha_1 \ , \qquad 10$$

where $\cos \alpha_1$ is the "new" elevation angle in the second layer. For this second layer, utilizing equation 7, we have

$$(r + h_o) \cos \alpha_1 = (r + h_o + h_1) \cos \beta \ ,$$

or

$$(r + h_o) \cos \alpha_1 = (r + h) \cos \beta \quad . \qquad 11$$

Again from Huygens' principle, we have

$$n \sin (90° - \alpha) = n_1 \sin (90° - \beta) \ ,$$

or

$$\cos \beta = \frac{n}{n_1} \cos \alpha \quad . \qquad 12$$

Substitution of equations 11 and 12 into equation 10 yields

$$\cos \alpha_o = \left(1 + \frac{h}{r}\right) \frac{n}{n_o} \cos \alpha \quad . \qquad 13$$

c. If the refractive index is assumed to vary linearly, for instance, as

$$n = n_o + gh, \qquad 14$$

where n_o is the surface refractive index, and g is the refractive gradient, then

$$\frac{n}{n_o} - 1 + \frac{gh}{n_o} \cong 1 + gh \quad . \qquad 15$$

The approximation in equation 15 is quite valid for practical values of the variables, since $n_o \cong 1$. Substitution of equation 15 into equation 13 yields

$$\cos \alpha_o = \left(1 + \frac{h}{r}\right)\left(1 + gh\right) \cos \alpha \quad . \tag{16}$$

Expansion of equation 16 yields

$$\cos \alpha_o = \left[1 + gh + \frac{h}{r} + \frac{gh^2}{r}\right] \cos \alpha \quad . \tag{17}$$

Within the brackets of equation 17, the term of gh^2/r may be neglected in comparison to the other terms, and we obtain

$$\cos \alpha_o = \left[1 + h\left(g + \frac{1}{r}\right)\right] \cos \alpha \quad . \tag{18}$$

In equation 18, if the term $(g + 1/r)$ is replaced by an equivalent radius as

$$\frac{1}{r'} = g + \frac{1}{r} \ , \tag{19}$$

or

$$r' = \frac{r}{1 + gr} \quad , \tag{20}$$

equation 18 can be rewritten as

$$\cos \alpha = \left(1 + \frac{h}{r'}\right) \cos \alpha \quad . \tag{21}$$

d. Equation 21 is identical in form with the previous equation 7 for rectilinear propagation in a homogeneous troposphere. Therefore, if the appropriate radius factor, r', is utilized, propagation paths in an inhomogeneous atmosphere can be represented as ray paths, whenever the refractive index variations can be represented approximately as expressed in the previous equation 14.

For a standard atmosphere, g = -39 N units/km. Substitution of this value in equation 20, with the real earth radius (r = 6410 km) yields

$$r' = \frac{6410}{1 - 39 \times 6410 \times 10^{-6}} = 8547 \text{ km} \quad . \qquad 22$$

The value of r' in equation 22 is approximately equal to 4/3 r. This demonstrates the origin of the 4/3 earth radius factor for rectilinear path construction in a standard atmosphere. For the value of $g_1 = -10$ N units/km and $g_2 = -80$ N units/km, the corresponding radius factors are $r_1' \cong 6849$ km and $r_2' = 13157$ km.

6. In the previous Figure 1, the height y (for the tangent path) is often called the earth's depression. If a transmitter is located at point A, with a zero elevation angle, the propagation path is along the line D. From the right triangle involving D, r and y in Figure 1, we have

$$(r + y)^2 = D^2 + r^2 \quad . \qquad 23$$

Expansion of equation 23 yields

$$r^2 + 2ry + y^2 = D^2 + r^2 \quad ,$$

or

$$2ry + y^2 = D^2 \quad . \qquad 24$$

For practical values of the variables in equation 24, the term y^2 can be neglected, and we obtain

$$y = \frac{D^2}{2r} \qquad 25$$

Equation 25 is accurate to better than 0.2% for D values as large as 500 km.

Equation 25 is a parabola,

$$y = kD^2 \quad . \tag{26}$$

If y is expressed in meters and D is expressed in kilometers, then the proportionality constant k, for a standard atmosphere, is

$$k = \frac{10^3}{2 \times 8547} \cong 0.0585 \cong 1/17 \quad . \tag{27}$$

The parabolic representation is useful in plotting path profiles and ray paths for tropospheric and diffraction paths.

7. With reference to Figure 1, it is noted that all propagation path distances may be represented by the distance value of D in equation 26. This results because any transmitter elevation angle α_o is always small, and path distances (either along the earth's surface, or along D in Figure 1, or from point A to point B in Figure 1) are small compared to r or r'. Therefore, sufficient accuracy is maintained by equation 26 for any practical values of y and D, including situations where $\alpha_o \neq 0$.

8. The development of relationships between distance measurements over a real earth surface and a fictitious earth surface are sketched as follows.

a. In Figure 3, the real earth surface is indicated with a radius r. A transmitter of height h is assumed to be located at point A, which is some distance S along the earth's surface from point B. The distance and height are such that the convex propagation path, p, from point A is tangent to the earth's surface at point B. The propagation path p is indicated to have a curvature equivalent to the radius R, for a standard atmosphere. It has already been established that this path will map into a straight line (ray path), if an earth radius factor of r' = (4/3)r is utilized.

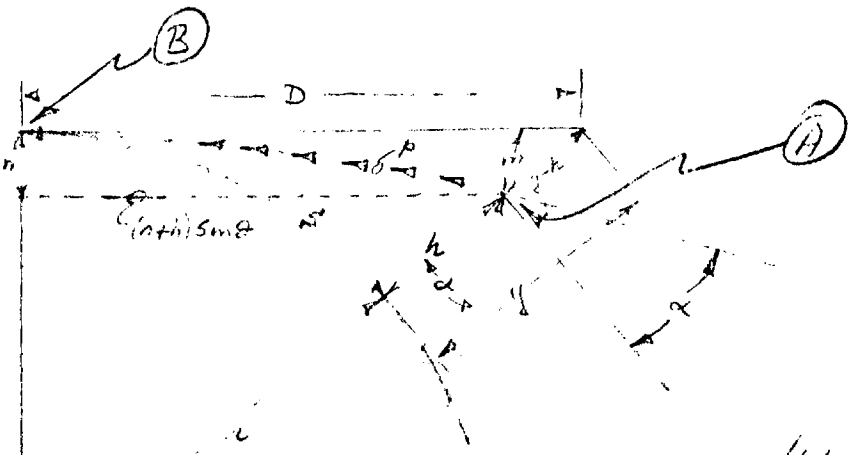

$$\left(1+\frac{h}{r'}\right)\cos\alpha = 1$$

$$m = \frac{(y-h)\cos\theta}{\cos(\theta-\alpha)}$$

$$n = m\cos(\theta-\alpha)$$

$$y = r\frac{(1-\cos\theta)}{\cos\theta}$$

Figure 3
Path Curvature for Standard Atmosphere

b. Since the propagation path at point B is tangent to the earth's surface, $\alpha_o = 0$, $\cos \alpha_o = 1$, and from the previous equations 21 and 22,

$$\left(1 + \frac{h}{\frac{4}{3}r}\right) \cos \alpha = 1 \quad , \tag{28}$$

or

$$\cos \alpha = \frac{1}{1 + \frac{3h}{4r}} \quad . \tag{29}$$

For small angles and since $\frac{3h}{4r} << 1$, equation 29 can be rewritten as

$$1 - \frac{\alpha^2}{2} = 1 - \frac{3h}{4r} \quad ,$$

or

$$\alpha^2 = \frac{3h}{2r} \quad . \tag{30}$$

c. The value of R may be determined as follows.

$$\sin(\theta - \alpha) = \frac{(r+h) \sin \theta}{R} \quad , \tag{31}$$

and

$$\cos(\theta - \alpha) = \frac{R - r(1 - \cos \theta) + h \cos \theta}{R} \quad . \tag{32}$$

Substitution of equation 32 into equation 31 and solution for h yields

$$h = R(\cos \alpha - \cos \theta) - r(1 - \cos \theta) \quad . \tag{33}$$

For small angles equation 33 may be rewritten as

$$h = \frac{\theta^2}{2}(R - r) - \frac{R\alpha^2}{2} \quad . \tag{34}$$

d. Substitution of equation 34 into the previous equation 30 yields

$$\alpha^2 = \frac{3\theta^2(R - r)}{4r + 3R} \quad , \tag{35}$$

or

$$\alpha = \theta \sqrt{\frac{3(R - r)}{4r + 3R}} \tag{36}$$

Finally, if equation 33 is substituted into equation 32, and the result is solved for R, we obtain

$$R = \frac{r \sin \theta}{\sin \theta - \sin \alpha} \tag{37}$$

For small angles, equation 37 may be rewritten as

$$R = \frac{r\theta}{\theta - \alpha} \tag{38}$$

Substitution of equation 36 into equation 38 yields

$$R = \frac{r}{1 - \sqrt{\frac{3(R - r)}{4r + 3R}}} \quad ,$$

or

$$R = 4r \tag{39}$$

Therefore, the radius of curvature for the convex propagation path, p, in Figure 3, is equal to 4r.

e. The real earth and propagation path p shown in Figure 3 have been shown in their parabolic representation in Figure 4(a). This representation has been established above in paragraph 6. The smooth earth surface

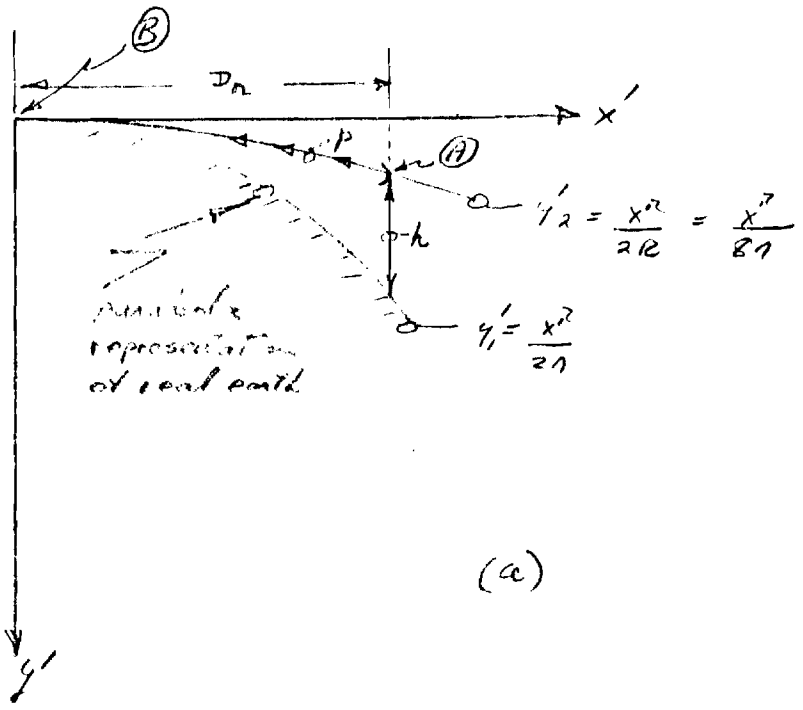

(a)

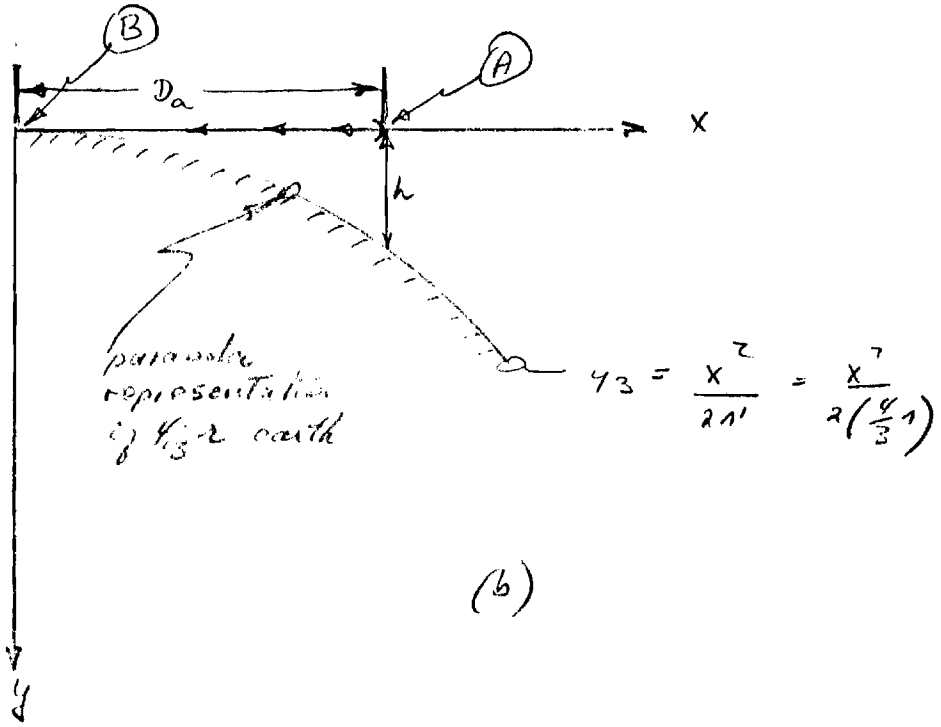

(b)

FIGURE 4
Equivalent Path Plots

is indicated in Figure 4(a) as

$$y_1' = \frac{x'^2}{2r} \quad , \tag{40}$$

and the convex propagation path, p, as

$$y_2' = \frac{x'^2}{8r} \quad . \tag{41}$$

The following transformation,

$$\left.\begin{aligned} y' &= y + \frac{x^2}{8r} \\ x' &= x \end{aligned}\right\} \quad , \tag{42}$$

will map the real earth plot shown in Figure 4(a) into the 4/3 earth plot shown in Figure 4(b). For instance, substitution of equation 42 into equation 40 yields

$$y_1' = y_1 + \frac{x^2}{8r} = \frac{x'^2}{2r} = \frac{x^2}{2r} \quad ,$$

or

$$y_1 = \frac{x^2}{2\left(\frac{4}{3}r\right)} \quad . \tag{43}$$

Equation 43 represents the mapping of the real earth in Figure 4(a) into a fictitious earth with $r' = \frac{4}{3}r$ in Figure 4(b). Also, substitution of equation 42 into equation 41 yields

$$y_2' = y_2 + \frac{x^2}{8r} = \frac{x'^2}{8r} = \frac{x^2}{8r} \quad ,$$

or

$$y_2 = 0 \quad . \tag{44}$$

Equation 44 represents the mapping of the convex propagation path, p, in Figure 4(a) into a straight line (path D_a) in Figure 4(b).

f. Finally, the point A in Figure 4(a) is assumed to be located such that for the indicated antenna height h and the path distance D_r, the convex propagation path, p, is tangent to the earth's surface at point B. From construction in Figure 4(a),

$$h = y_1' - y_2' \quad ,$$

or

$$h = \frac{D_r^2}{2r} - \frac{D_r^2}{8r} = \frac{D_r^2}{2\left(\frac{4}{3}r\right)} \quad . \qquad 45$$

If the same antenna height h (as indicated in equation 45) is utilized in Figure 4(b), we have

$$y_3 = \frac{D_r^2}{2\frac{4}{3}r} = \frac{D_a^2}{2\left(\frac{4}{3}r\right)} \quad . \qquad 46$$

or

$$D_r = D_a \quad . \qquad 47$$

Equations 45 and 47 represent the fact that linear measurements for the real earth representation are invariant under the transformation to the fictitious earth representation.

9. It may be interesting to note the effects of different refractive index gradients. The representations given thus far relate to a standard atmosphere with g = -39 N units/km and r' = (4/3)r. For g = -10 N units/km, r' = 6849 km, as established above in paragraph 5d. Therefore, a greater antenna height would be required if the same distance D_a (= D_r) were to be

utilized as depicted in Figure 4(b). Thus

$$y_4 = \frac{D_r^2}{2r'} = \frac{D_r^2}{2 \times 6849} \quad ,$$

or

$$y_4 \cong 0.0730 D_r^2 \qquad 48$$

For a standard atmosphere, from the previous equation 46, we had

$$y_3 \cong 0.0575 D_r^2 \qquad 49$$

Hence,

$$y_4 \cong 1.25\, y_3 \qquad 50$$

On the other hand, if the same antenna height were maintained and the refractive gradient changed from -39 to -10 N units/km, the radio horizon distance D_a would be determined as follows. For a standard atmosphere, from equations 45 and 46

$$y_3 = h = \frac{D_r^2}{2r'} = \frac{D_r^2}{2\left(\frac{4}{3}r\right)} \qquad 51$$

For g = -10 N units/km, r' = 6849 km, then

$$y_3 = h = \frac{D_a^2}{2r'} = \frac{D_a^2}{2 \times 6849} \quad . \qquad 52$$

Hence,

$$D_a^2 \cong 0.801\, D_r^2 \quad , \qquad 53$$

or, in the general case,

$$D_a^2 = \frac{r_2'}{r_1'} D_r^2 \quad , \tag{54}$$

where r_1' and r_2' represent, respectively, a standard and a nonstandard atmosphere radius, and where D_r and D_a represent, respectively, a standard and a nonstandard atmosphere distance. Therefore, for a change $\Delta g = +29$ N units/km (i.e., $g = -10$ N units/km),

$$D_a \cong 0.89\ D_r \tag{55}$$

Similarly for a change $\Delta g = -41$ units/km (i.e., $g = -80$ N units/km),

$$D_a \cong 1.24\ D_r \tag{56}$$

Equations 55 and 56 indicate that refractive index changes can cause significant changes in path distances, particularly, for path clearance over the earth surface or over obstacles. Even for a relatively small change in the refractive gradient of +10 N units/km (i.e., $g = -29$ N units/km), there results a change in the radio horizon distance of 4.6% for an antenna height of 49 meters, or a change in antenna height of 8.5% for the same radio horizon distance of 29 km. The latter change would represent approximately a loss of 4.2 meters clearance at the horizon. For a clearance of the first Fresnel zone at a frequency of 5000 MHz ($\lambda = 5$ cm), and a distance of 29 km, the midpoint of the first Fresnel zone occurs at a height L as

$$L = \frac{\sqrt{\lambda d}}{2} \quad , \tag{57}$$

or

$$L \cong 20.8 \text{ meters} \quad . \tag{58}$$

As mentioned above, the increased refraction for $\Delta g = +10$ N units/km amounts to a reduction in clearance at the horizon of about 4 meters. This reduction is equivalent to a loss of about 20% of the first Fresnel zone clearance in the example given.

10. For frequencies above 50 to 100 MHz, communication links may be classified arbitrarily into three types. These are depicted as a line-of-sight (LOS) path in Figure 5(a), and as a diffraction path and a tropospheric scatter path in Figure 5(b).

a. In Figure 5(a), a real earth radius plot is indicated. The antenna is located at point A with a height h above the earth's surface. The optical line of sight is indicated to be tangent at point B and the radio horizon is indicated at point C. The optical path is approximately equal to 0.9 of the propagation path p. For LOS paths, the receiver antenna is usually located within optical sight of the transmitter antenna. Thus, LOS paths generally refer to unobstructed optical paths. Path distances are usually restricted to 60 km or less. As an example, radio relay communication networks utilize such paths. Complicating factors for any given link are due primarily to multiple reflections from the earth's surface along the propagation path.

b. In Figure 5(b), a 4/3 earth radius plot is indicated. For a transmitter located at point A, a spherical diffraction path is shown to propagate over the transmitter radio horizon (point C), over a smooth earth surface to the receiver radio horizon (point D), and on to the receiver at point E. Diffraction path communications generally relate to one of several different path types, all of which are non-optical. Thus, propagated energy may be diffracted over an obstacle (for instance, a mountain range).

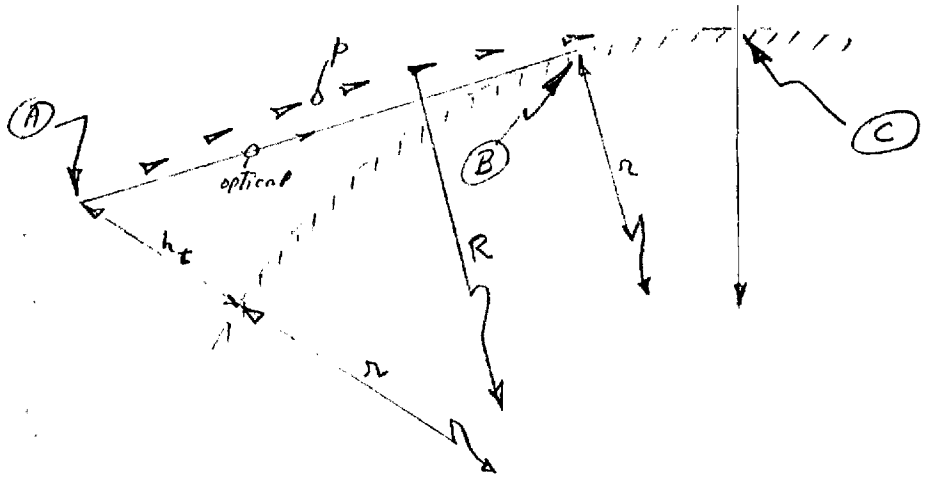

(a)

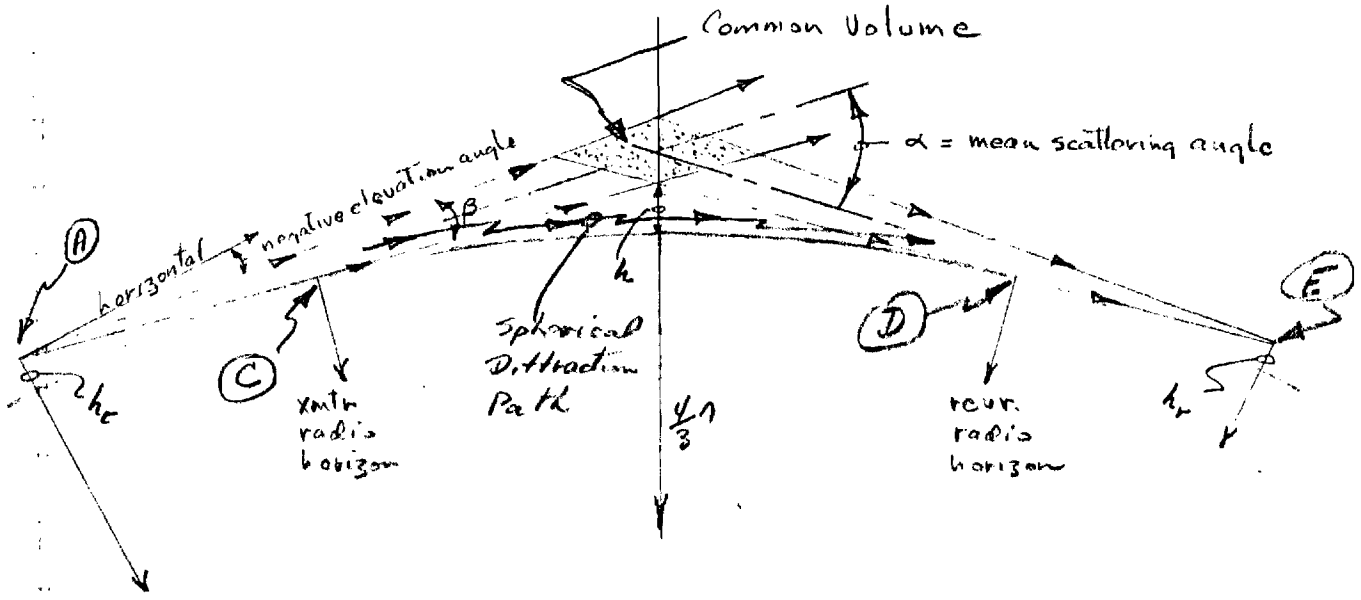

(b)

FIGURE 5
Types of Propagation Paths

Also, energy may be diffracted around or over an extended surface (for instance, spherical diffraction over the earth's surface, as depicted in Figure 5b). Diffraction signal levels are rapidly attenuated beyond the radio horizon, and path distances are usually restricted to 200 km or less. Complicating factors for any given link are generally associated with the initial installation of the link and the initial prediction of received signal strength. The complications may arise from the difficulty in a proper determination of an appropriate diffraction path. This is particularly true for spherical diffraction over rough or mountainous terrain. However, subsequent to a successful installation, received signal levels are generally rather stable with respect to signal variations. Stability may be further enhanced, if any refractive index changes are not sufficiently large such that the transmitter beam could be shifted downward to produce inadequate clearance (tending to blockage of the radiation, as mentioned above in paragraph 9).

c. Far-beyond-the-horizon communications generally relate to tropospheric scatter paths in the frequency bands considered. Path distances are usually less than 700 to 900 km, but have been established over significantly larger distances; i.e., 2500 miles.[3,4] A typical tropo path is shown in Figure 5(b). An appropriate equivalent earth radius should be established, for instance, from the previous equation 20, utilizing the mean value of g which is expected for the tropo path in question. In Figure 5(b), a 4/3 earth radius plot is indicated for a standard atmosphere (g = -39 N units/km). (An equivalent parabolic representation would be more useful in actual path construction, since obstacle heights can be readily indicated.)

(1) In Figure 5(b), the ray path from the transmitter antenna through the transmitter radio horizon is constructed. A similar path is constructed from the receiver antenna. The intercept of these two ray paths defines the lower extent of the common volume, shown as the shaded area in Figure 5(b). If the antenna beam width, β, is assumed to be the same for both transmitter and receiver, the corresponding ray paths for the specified beam width can be constructed as shown. The intercept of these latter two ray paths defines the upper extent of the common volume. It should be noted that the common volume, as shown in Figure 5(b), appears greatly foreshortened in its lateral extent. This is because of the distortion in the vertical scale factor. In actual practice, the common volume will extend generally from the vicinity of the transmitter radio horizon to the vicinity of the receiver radio horizon.

(2) In actual path construction, a parabolic representation is recommended. Then, the first ray paths constructed would extend from the transmitter and receiver antennas to the tangent points on the highest obstructions at the respective radio horizons.

(3) Propagated energy from the transmitter may be scattered and/or reflected from atmospheric constituents within the common volume and redirected towards the receiver antenna.

(4) The mean scattering angle, α, is shown in Figure 5(b) as the angle between the antenna beam centers. The majority of the radiation from the transmitter propagates through the common volume into space. Only a small part of the energy is redirected toward the receiver antenna. The redirected energy is a function of the scattering angle and decreases rapidly as α increases. Therefore, antenna elevations need to be

as large as possible. In particular, it is desirable to have a clear unobstructed path to the radio horizon, such that negative antenna elevation angles can be utilized. As is evident from construction in Figure 5(b), both negative antenna elevation angles and increased antenna heights will decrease the scattering angle for any given link configuration.

(5) Complicating factors for any given tropo link may be classified in two areas: initial prediction of mean received signal level; and subsequent establishment of received signal levels (including signal variations) for satisfactory communications on the link. Both areas are related to the variability of the atmospheric characteristics (primarily within the common volume) which generate the scattered and/or reflected signals incident at the receiver.

(6) For any given tropo link, it is noted that some energy is propagated to the earth's surface all along the tropo path, and may extend well beyond the receiver terminal. The transverse extent of this energy along the propagation path is limited primarily by the transmitter beam width, although scattering may cause an apparent beam widening of a factor of 2 or more.[5,6,7] Antennas utilized with troposcatter equipment usually have small beam widths ($\leq 2°$). Consequently, the illuminated earth surface along a tropo path may appear in the form of a greatly elongated elliptical area, with major axis in the path direction.

d. Finally, it is noted that some particular communication link may be described as consisting of both a diffracted path and a tropo path. For instance, the path length shown in Figure 5(b) could represent a path distance between 100 and 200 km. This distance might be considered as a "long" diffraction path or a "short" tropo path. Consequently, the received

signals may result from two basically different components: one part may occur from a diffracted signal; and the second part may occur from the tropo scattered signal. For such path distances, it may be desirable to include signal level predictions from both path sources.

B. Review of Theories

1. The detailed mechanisms which cause (or enable) far-beyond-the-horizon propagation are not completely understood. The terminology commonly applied is "tropospheric scatter" propagation. This is somewhat misleading since, in addition to scattering, the mechanisms of partial reflections can constitute a major contributing factor.

2. Within the troposphere many different variations exist in the physical characteristics, including a marked variation in the quantity of one of the constituents, namely water vapor. These variations are both time and space dependent. The principal parameters are labeled as temperature, humidity, density, pressure, and air stability.[3] In the communication bands of interest (above 100 MHz), these variations may appear as gradual (relatively smooth) changes or they may appear as abrupt (apparently discontinuous) changes. The degree of change depends on operating frequency as well as on the type of atmospheric conditions which are prevalent. A principal measure of some of these variations is contained in the refractive index variations. In particular, the detailed variations of the refractive index with height can be most useful in ascertaining troposcatter path characteristics.

3. An example of a radiosonde recording is sketched[8] in Figure 6. It is apparent that at least two different situations can be defined. In the figure, these situations have been labeled as turbulent layers and as stable layers (or stable discontinuities). For the purpose of discussion, the troposphere is classified arbitrarily into two different types (or situations) of air movement: turbulent layers and stable layers. These two types may be considered to exist separately in space and time. Generally, the two types may be interspersed. Thus, turbulent layers of air may be interspersed generally with thinner stable layers of air.

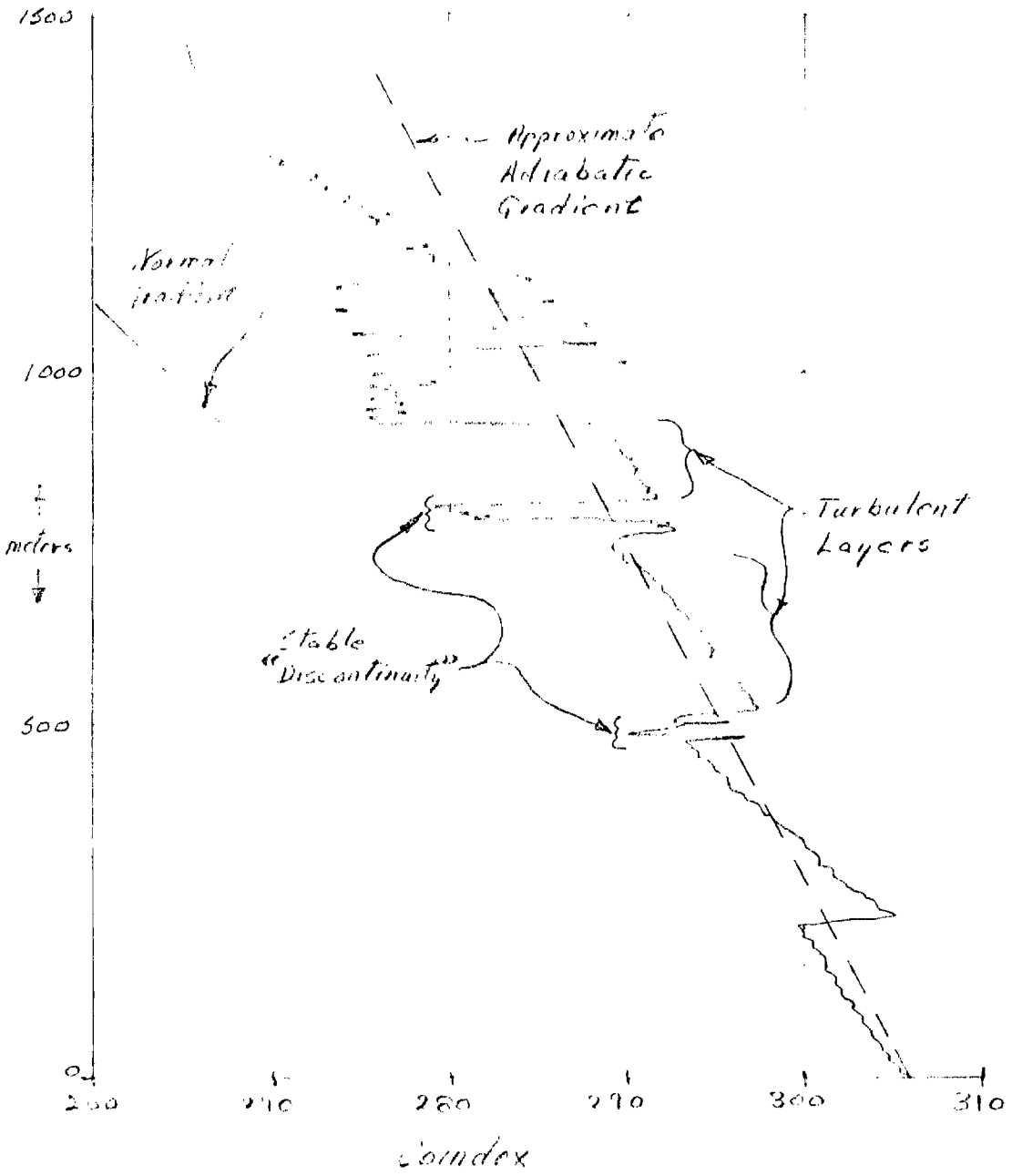

FIGURE 6

Refractive Index Variations

4. A turbulent air layer may be characterized by relatively rapid-flowing eddy currents which cause relatively rapid mixing of the air. Within a turbulent layer, the temperature gradient may approach that of the adiabatic gradient[9] ($\sim -10°C/km$). The diffusion of water vapor is relative rapid. Hence humidity variations within a turbulent layer are relatively small.

a. Turbulent layers are envisioned as the "source" of forward-scatter radiation. There are a number of theories related to the mechanisms involved which can cause scattering. Somewhat different functional relationships may be derived between the refractive index and the dimensions of the turbulent layer and the dimensions of the elementary scatterers.[10,11,12,13,14]

b. The power scattered at some angle θ (measured from the incident radiation) will depend on the assumption of some particular spatial distribution of the turbulence. However, the implication results that the scattered radiation varies in intensity proportional to θ^{-4} or θ^{-5}. Frequency effects are also indicated, where the scattered power (relative to free space) may be proportional to λ, $\lambda^{-1/3}$, λ^{-1}, or even λ^{-2}. Generally, the proportionality of λ appears to be in better agreement with experimental results (Reference 9, page 147). If the mean scattering angle θ ($= \alpha$ in Figure 5(b)) is assumed to be proportional to path distance D, the scattered power is proportional approximately to D^{-6}. (The assumption of proportionality between θ and total path distance D is valid for near zero elevation angles.)

c. The refractive index variations within a turbulent layer are of the order of a few N units (Reference 9, page 30). A representative scale of turbulence is of the order of tens of meters in thickness (vertical extent). The functional dependence of the refractive index with height (within a turbulent layer) may be proportional to h^{-2} or its form may be exponential.

5. A stable layer is associated with laminar air flow. The thickness (vertical extent) of stable layers is quite variable, and very thin layers may exist. These thin layers are called "feuillets" in French (Reference 9, page 26) and may vary from a few meters to several tens of meters in thickness. The temperature gradient can be quite variable, particularly across layer boundaries, where apparent discontinuities may appear. Water vapor diffusion is relatively slow (due primarily to gravity). Hence, humidity variations within a stable layer may be relatively large. Humidity variations across layer boundaries may appear discontinuous.

a. Stable layers are envisioned as the "source" of partially reflected radiation. Dependent on the layer dimensions, including surface curvature characteristics, diffuse and/or specular reflection can occur. Diffuse reflection relates to reflected energy from elemental surfaces, the reflected components being in a random phase relationship. Specular reflection relates to reflected energy whose components are in some particular phase relationship; thus, constructive or destructive interference can occur.

b. Reflected radiation appears to vary in intensity proportional to θ^{-5} or θ^{-6}. Frequency effects are indicated to be proportional to λ^3 and λ^2, respectively, for specular and diffuse reflection components.

c. If the mean reflection angle θ is assumed to be proportional to path distance, reflected power is proportional to D^{-7} and D^{-6}, respectively, for specular and diffuse reflections.

d. Within a stable layer, refractive index variations may be of the order of a few hundredths of an N unit (Reference 9, page 32) larger variations, as well as apparent discontinuities can occur across layer surfaces.

6. The previous Figure 6 exemplifies these different situations of air movement. Although there does not appear to be a general agreement between the proponents of the various theories for troposcatter propagation, suffice it to say that at least two basically different modes are apparent. Historically, scattering theories were first developed. Partial reflection theories were developed more recently.

a. Scattering theory predicts a relatively larger area of ground illumination than reflection theory. In addition, larger path distances are predicted from scattering theory for the same received signal level as compared to reflection theory predictions. This latter prediction results from the proportionalities of $1/D^6$, or $1/D^7$, and $1/f^2$, or $1/f^3$ from reflection theory as compared to $1/D^6$ and $1/f$ from scattering theory. However, for path distances greater than 300 or 400 km, the reflection mode may predominate. This can result because of a general tendency towards larger numbers of stable layers at the higher elevations. Thus, as path distance increases, the upper limit of the common volume increases in height, and a larger number of these stable layers are included. As the number of stable layers increases in comparison to the number of turbulent layers, the reflection mode may predominate over the scattering mode.

b. Reflection theory predicts a relatively smaller area of ground illumination than scattering theory. The illuminated area tends to the shape of a greatly elongated and narrow ellipse, parallel to the path. This results from diffuse reflection. When specular reflection exists, the above mentioned elliptical area may contain "bright" spots which are representative of the more intense specularly reflected signals resulting in constructive interference.

7. To some extent these mechanisms of scattering, diffuse reflection, and specular reflection have been indicated from experimental evidences. Signal analyses have been performed in several experiments relating to instantaneous spatial distribution and to instantaneous frequency distribution. These analyses[6,7,15,16] support the existence of the above modes.

8. There appears to exist yet a third possible interpretation for the troposcatter phenomena. Other theorists[3,17,18] maintain that troposcatter communications can be explained satisfactorily by an appropriate application of diffraction theory. The more common applications of diffraction theory to long-distance paths calculate spherical diffraction around the earth in a homogeneous troposphere. Such applications predict signal attentuations which appear correct for distances to the order of 150 km. However, for larger distances, the predicted signal attenuations are much greater than those observed experimentally. It has been stated that such applications are erroneous by virtue of an incorrect choice of model; i.e., a homogeneous troposphere. Proponents of the diffraction theory of modes assume the troposphere to be stratified in accordance with the law of gravity. Long-distance propagation then can be interpreted as a result of "wave ducting." Thus, propagation is considered as occurring in a guided mode within the total layer of the troposphere, due to coherent diffusion of the radiation by the polarizable molecules in the air. The developed wave functions of the wave equation are sufficiently precise such that the different modes of propagation can be added vectorially. (The modes are the mathematical expressions for coherent diffusion.) When the modes are summed to high order, the predicted attenuation at large distances is very much less than that obtained from a

homogeneous tropospheric representation. Different assumptions with respect to the mean refractive index profile with height produce somewhat different results. Profiles in the form of a finite exponential, an inverse quadratic, or a bilinear model have been utilized. Predicted signal levels are of the same order as those obtained experimentally.

9. It is interesting to note that the diffraction mode theory yields predicted signal levels without any assumptions with respect to specific tropospheric inhomogeneities (such as turbulent and stable layers). Also, it should be noted that at large distances (> 721 miles), the lowest part of the common volume lies above the troposphere (> 12 miles high). Therefore, at larger distances scattering and/or reflection theories predict rapid increases in signal attenuation. However, these predicted results do not appear to agree with some experimental observations. For instance, an experimental troposcatter link[3,4] has been generated between the California coast and Hawaii, i.e., a path distance of ~2500 miles. It does not seem reasonable to project an appreciable amount of the tropospheric constituents into the stratosphere, such that the concept of turbulent and/or stable layers can exist and enable these long ranges of tropo links based on the scattering and/or reflection mechanisms. (Other investigators maintain that these excessive ranges can be explained not on the basis of the diffraction mode theory but on the basis of elevated ducting of the propagating energy).

C. Theoretical and Empirical Approaches

1. The authors of the diffraction theory of modes suggest that this theory adequately explains all trans-horizon propagation, including both diffraction and troposcatter. Although this position may be correct, this theory does not appear to be sufficiently developed to explain some of the observed effects from localized meteorological conditions over a given tropo path. For instance, the existence of turbulent and stable layers appears to be well documented. In addition, experimental observations and signal analyses indicate that received tropo signals of the type expected from scatter theory and from reflection theory also exist.[6,7,15,16] Finally, when turbulent tropospheric conditions prevail, received signals exhibit the principal characteristics associated with scatter theory. These observations include the fact that the rapid amplitude fluctuations of the signals obey a Rayleigh distribution, which is predicted from scatter theory (Reference 9, page 149).

2. It is concluded, therefore, that no single theory adequately explains all of the major phenomena associated with troposcatter propagation. Rather, there appear to be a number of different mechanisms (associated with the different basic theories) any one of which may become prevalent over a given tropopath, dependent on meteorological conditions. Therefore, it seems unreasonable at this time to attempt a purely theoretical explanation of received signal strengths. On the other hand, it is considered possible to provide empirical relationships which may predict mean signal levels in a satisfactory manner.

3. Furthermore, it is considered mandatory that simple yet adequate

means should be provided for computation of troposcatter signals for any given link configuration. The expanding utilization of troposcatter communications demands a satisfactory solution. In addition, tropo communication networks require satisfactory solutions if the available frequency spectrum is to be utilized in an efficient manner. This brief study has attempted to ascertain a "best" approach for signal level predictions in tropo networks which, at the same time, will enable efficient and conservative use of the available frequency spectrum. This study has not been completed. However, sufficient work has been accomplished which indicates some apparently fruitful avenues of approach.

4. There are a number of empirical relationships which have been developed by various authors, most of which are based on experimental results as well as one or more of the underlying theories.[19,20,21,22,23,24] Specific empirical relationships are discussed and applied in the next section. The remaining paragraphs of this section relate to basic information and procedures which will be incorporated into a proposed approach for estimating received tropo signal levels.

5. All received signals which are involved in propagation through space exhibit statistical variations. Therefore, on any given tropo link for any given time period, the received signal levels will be related to mean signal levels with appropriate standard deviations. A particular mean signal level will be representative of the expected signal level, based on some type of signal averaging over a given time period. For instance, the median value is the mean signal value which is expected to occur for 50% of the time. If the mean signal level is based on a monthly time period, the

median value of this mean signal is that level of signal which may be exceeded for 50% of the time during one month. If an hourly mean value is utilized, the median value is that level of signal which may be exceeded for 50% of the time during one hour. Correspondingly, the 99% value is that value of mean signal level which may be exceeded for 99% of the time (for the specified time period). More often, the 99% values (or sometimes the 99.9% values) are utilized as expected signal levels for the establishment of satisfactory communications. For a given mean signal value, the difference in the signal levels between the 50% value and the 84% value establishes the standard deviation σ. The difference between the 50% and 90% values is representative of 1.286σ, while the difference between the 50% and 99% values is representative of 2.326σ.

6. For the purposes of discussion, received tropo signals may be classified into different types. Mean signal levels may be related to long term and short term signal levels. Also, the signal variations may be related to long term, short term, and rapid types.

a. Long term signals relate to mean signal values which have been established by some type of signal averaging over a relatively long time period. Generally, a long term mean value may be characterized according to the locale of a tropo link. Correspondingly, signal values may be further classified as to seasonal, monthly, or diurnal mean values. More detailed discussions are given in the following paragraph 8.

b. Long term signal variations relate to the difference in mean values, for instance, between seasons, months, or during a diurnal period.

c. Short term signals also can relate to mean signal values

averaged over a short period of time, for instance, hourly mean values. Generally, an hourly mean value will relate to worst-case conditions, i.e., the most unfavorable hour during the diurnal period, which occurs during the most unfavorable month in the most unfavorable season for propagation.

d. Short term signal variations may relate to standard deviations in the hourly mean values, determined from prior experience. On the other hand, short term signal variations will also occur as a result of localized storms, weather fronts, and the formation and dispersion of temperature inversions (ducts), etc. In the latter cases it is often difficult to ascribe standard deviations.

e. Rapid signal fluctuations can relate to the particular type of meteorological conditions which are prevalent. Signal fluctuations may vary from several cycles per second to the order of minutes. As has been mentioned, when turbulent meteorological conditions prevail, the predominant mode for troposcatter propagation is by means of the scattering mechanisms. Also, the statistical distribution of the rapid amplitude fluctuations of these signals obeys a Rayleigh distribution. When more stable meteorological conditions prevail, received signals exhibit both scattering and reflected signal characteristics. The rapid fluctuations are characteristically less dispersed than a Rayleigh distribution. These latter fluctuations often can be approximated by the superposition of one or more relatively stable amplitude vectors together with a Rayleigh distributed vector.

(1) A random variable which can possess only discrete, positive integer values (the total number of values being finite), will be subject to a Binomial distribution. If the number of values tends to

infinity as the probability of a given value tends to zero (the product of the number of values and the probability being equal to a constant), the distribution is that of Poisson. If a random variable can possess continuous values, but all values are not equally probable, the distribution is expressed by the Laplace-Gauss law (Normal law). The probability of this distribution for any value x, with a mean value m, and a standard deviation σ, can be expressed as

$$P(x) = \frac{1}{\sigma\sqrt{2\pi}} \int_{x}^{\infty} e^{-(x-m)^2/2\sigma^2}\, dx. \qquad 59$$

In equation 59, if the variable x is exponential in character, and is measured in db, the resultant distribution is labeled as log-normal.

(2) If tropo signals are assumed to result from a large number of scattered signals, it can be shown (Reference 9, page 173) that the received signals obey a Rayleigh distribution as

$$p(r) = e^{-r^2 / k^2}, \qquad 60$$

where P(r) is the probability of a given amplitude value r, and k is the mean value.

(3) A sketch of the Rayleigh distribution and log normal distributions for several values of standard deviations are shown in Figure 7 (Reference 9, Chart S). As previously mentioned the standard deviation is the difference in the values of the variable (relative amplitude) at the 50% and 84% levels or at the 16% and 50% levels.

(4) When a given vector is superimposed on a large number of vectors of random phase, the resultant distributions are sketched in Figure 8 (Reference 9, page 175). These plots are somewhat representative

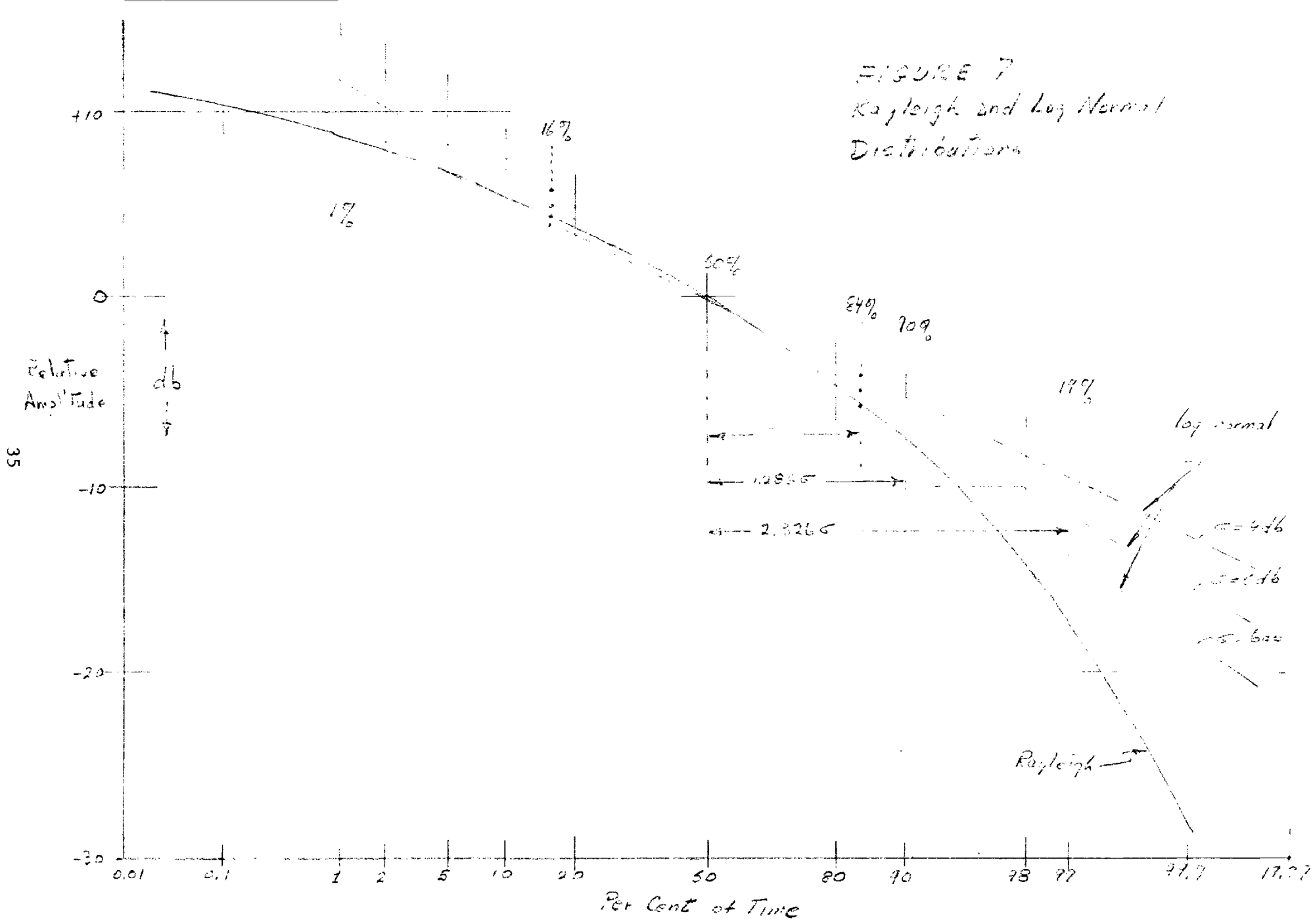

FIGURE 7
Rayleigh and Log Normal Distributions

of the situations existent with a diffuse reflection signal superimposed on scattered signals. The several values of m represent several different ratios of the squares of the amplitudes of the given vector to the random vectors. A similarly shaped plot is obtained for a given vector and a large number of vectors whose phases are random within specified phase intervals. The Rayleigh distribution is obtained when the phase interval is $\pm \pi$.

(5) A given mean signal level (for a tropo link in a given locale), representative of the expected signal for a given time period, will exhibit a statistical distribution about the median (50%) value. Thus, the percentile plot of the given mean signal level will also be representative of the expected signal fluctuations (standard deviation). An example[5] is sketched in Figure 9, for several tropo links in the Northeastern United States (Also reference 9, page 65). A common transmitter (420 MHz) was utilized for the several different path lengths. The standard deviation for the 150 km path is about 5.4 db. This value decreases as the path distance increases to a value of about 2.3 db for the 900 km path.

(6) There does not appear to be any systematic relationship between signal fluctuations and mean signal levels. On the other hand, there exists the tendency toward a Rayleigh distribution with increased distance or with increased frequency. The rate of fading may be related to the number of signal fluctuations whose transits cross a specified level during a given time interval. Generally, the fading rate increases as frequency increases. However, the mean fading rate does not appear to change in any systematic manner with path distance. In addition, fading rate does

FIGURE 9

HOURLY MEDIANS

(Winter – temperate climate)

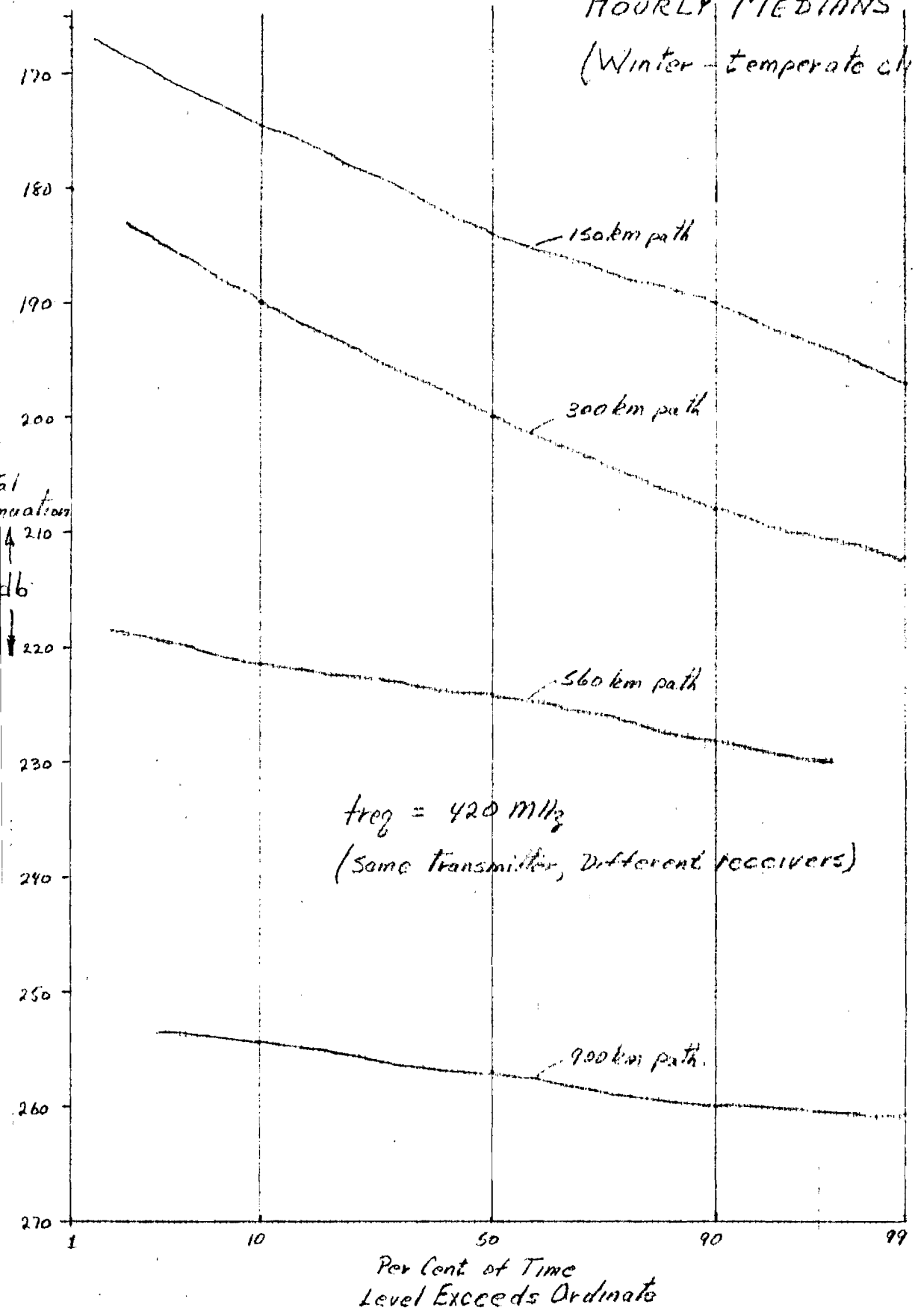

not appear to change in any systematic manner with signal level. On the other hand, fading rates are characteristically less rapid during stable tropospheric conditions.

7. Meteorological conditions overlying any particular tropo path appear as the principal variable affecting received signal levels. As has been mentioned, a composite measure of most of these tropospheric characteristics is contained in a detailed profile of the refractive index with height. Unfortunately, such data are not always available for any arbitrary tropo path. Therefore, in the development of a generally applicable procedure, refractive index data are not considered as a required input. On the other hand, the following two basic assumptions are applied in this study.

a. In general, more experimental data exist from troposcatter studies in the temperate climates of North America and Europe than in other climates. Therefore, a temperate climate will be utilized as a reference.

b. Troposcatter propagation by the mechanisms of scattering appears to be present to some extent for all meteorological conditions. Therefore, whatever the climate is, or whatever the tropospheric conditions are, the scattering phenomena will be utilized as a reference. In general, this procedure will establish a "worst-case" condition. This results because prevalent turbulent conditions over a tropo path usually produce minimal received signal levels.

8. The location of any given tropo path is considered arbitrary. For any arbitrary location, there is one common variable which may be utilized to categorize tropo paths for a general treatment. The common variable is climate. The various climatic conditions have been classified arbitrarily

into six types (Reference 9, page 75). The general tropo signal characteristics are listed in the following subparagraphs. The resultant empirical relationships are discussed in the next section.

a. In temperate climates, seasonal variations may be 15 db or more. This means that the mean signal levels can vary by 15 db (or more), primarily between summer and winter months. The greater attenuation (smaller signal level) occurs during winter months when turbulent conditions prevail. Monthly variations (σ) are about 4 to 6 db during winter and may increase to about 10 db during summer. Diurnal variations are about 4 db in winter and about 6 to 8 db during summer, maximum attenuation occurring in the afternoon. Generally, the magnitude of signal variations is greater for shorter paths and less for longer paths. An example has been shown in the previous Figure 9 for the distribution of hourly mean values for paths in the Northeastern United States. Attenuation with distance in temperate climates generally varies as D^{-7} with respect to free space. (If the free space dependence is included, attenuation generally varies as D^{-9}).

b. Desert climates have moisture contents which are relatively less than temperate climates, and turbulent conditions are generally more prevalent. Therefore, seasonal effects are generally smaller than in temperate climates, being about 8 db between extreme monthly values. Early summer months evidence the greatest attenuations, with a standard deviation of about 4 db. Diurnal variations are larger, being about 8 db between night and day, and the greatest attenuation occurs in the afternoon. The larger diurnal variations are probably associated with the generally larger temperature variations between night and day for a desert climate. Attenuation

with distance generally varies as D^{-8} with respect to free space. For a path length of 300 km, maximum signal attenuation in a desert climate may be 12 db greater than that for a temperature climate at the 99% value of the mean signal level.

c. Arctic climates generally are quite similar to desert climates. At any given distance, attenuation for an arctic climate may be about 2 db less than that for a desert climate.

d. Tropical climates generally exhibit larger seasonal variations than temperate climates. Seasonal variations often exceed 15 db and may be as large as 30 or 40 db or more. The dry season months produce the greatest attenuation. Monthly variations are erratic with standard deviations greater than 6 db. This erratic nature parallels the rapid and significant changes in meteorological conditions which are characteristic of tropical climates, i. e., storms, ducting, etc. In addition, diurnal variations are large and may exceed 25 db. The greatest attenuations usually occur in the afternoon. Attenuation with distance generally varies as D^{-7}, which is identical in form to that for temperature climates. However, at any given distance the maximum attenuation for tropical climates is less than that in temperate climates by about 5 db.

e. Equatorial climates generally exhibit less attenuation than tropical climates. This feature is compatible with the greater moisture content in equatorial climates. In addition, meteorological conditions are somewhat more stable in equatorial climates. Therefore, seasonal variations are smaller, being about 6 db. Maximum attenuation occurs during the rainy seasons. The monthly standard deviation is small, being about 3 db. Diurnal

variations are about 8 db, the attenuation being larger in the afternoon. Attenuation with distance generally varies as D^{-6} with respect to free space. For a path length of 200 km, maximum signal attenuation is about 7 db less than that for a temperate climate at the 99% value of the mean signal level.

f. The Mediterranean climate is contained geographically, of course, within the temperate zone. However, characteristics are significantly different than those for a temperate climate. Seasonal variations are about 25 db, with maximum attenuation occurring during the winter months. The standard deviation during winter months is about 6 db, and is greater during summer months. Diurnal variations are also larger, being about 10 db. Maximum attenuation occurs during the afternoon. Attenuation with distance generally varies as D^{-8} or D^{-9} with respect to free space. For a path length of 200 km, the maximum signal attenuation is about 5 db less than that for a temperate climate at the 99% value of the mean signal level.

9. As has been mentioned, the maximum attenuation of tropo signals is usually evidenced during turbulent meteorological conditions. Conversely, minimum attenuation is usually evidenced during anticyclonic conditions, i.e., when significant tropospheric stability is present. The simplest and most composite measure of these tropospheric characteristics is contained in the detailed profile of the refractive index with height. It should be obvious that a single index measurement (for instance, by radiosonde recording), may not be representative of the hourly, diurnal, monthly or seasonal variation. For useful applications, therefore, mean values of the refractive index must be established (or assumed from past measurements).

When such data are available, mean values of the refractive index (or gradient) may be utilized to correlate with or predict path attenuations. It should be noted that knowledge of the refractive index profile cannot be used theoretically to predict signal attenuations, since no general relationship is known. Attenuation predictions from refractive index data presently can be made only on a statistical basis with the aid of empirical relationships. However, in a given geographical area, if an empirical relationship has been established, then refractive index variations can be utilized to predict received tropo signal levels with reasonable accuracy. Some utilizations of refractive index data are mentioned briefly in the following subparagraphs.

a. The coindex and gradient values for a standard atmosphere have been given in the previous equations 3 and 4. As has been mentioned, a detailed knowledge of the mean refractive index profile can be utilized in a general way to predict prevalent meteorological conditions which affect received tropo signals. For instance, the evidences of turbulent and stable layers shown in the previous Figure 6 can yield quite useful (although indirect) information with respect to received signal levels. This is particularly true in applications of the empirical relationships and will be discussed further in the next section. Also, evidences of temperature inversions, duct formations, etc., may be ascertained from a refractive index profile.

b. The concept of an equivalent refractive index gradient has been tested in a limited number of situations. In general, an equivalent gradient can be defined as the mean value obtained between the surface value and that value at the height of the base of the common volume, for any particular tropopath. More often, mean gradient values are listed as the mean

value obtained between the surface value and the 1000 meter value. However, in the situations tested, a better correlation of attenuation with distance has been obtained by use of the equivalent gradient concept (Reference 9, page 79).

c. When mean values of the refractive index or gradient are not available, surface values may be utilized. For some cases variations of the surface value of the refractive index correlate with observed attenuations.[25, 26,27,28] However, in other cases, an inverse relationship exists. For instance, in Dakar (a tropical climate on the west coast of Africa) the mean surface value of the refractive index increases greater than 40 N units during the summer months; however, the mean gradient decreases from -90 N units/km to about -65 N units/km (Reference 9, page 100). For a given path length, the signal attenuation decreases with an increasing gradient (increasing in the sense of larger negative values of the gradient). In situations where the surface refractive index follows the same trend as the mean gradient values, utilization of the surface values of the refractive index will indicate the correct trend in signal attenuation. That is, an increase in the surface value of the refractive index is associated with a decrease in the signal attenuation. In the above cited example of Dakar, the reverse is true.

d. The extreme values of the surface index for February and August have been plotted by the National Bureau of Standards for the entire earth's surface, in the form of iso-index contours. In addition, iso-gradient contours for the major continents have been recorded.[29] These are mean gradient values determined from the surface and 1000 meter values. More detailed iso-index contours are available for the continental United States.[30]

e. When the tropospheric conditions are not representative of a standard atmosphere, or when variations in the refractive index (or gradient)

occur over a given tropopath, corrections can be made with respect to predicted effects on signal attenuation. However, until further study is completed, these correction terms should be applied only in temperate climates. The following relationships have been established by international agreement.[31]

$$\Delta A = 0.5\ (g' + 40) \qquad 61$$

or

$$\Delta A = -0.2\ (N-310) \qquad 62$$

In equation 61, ΔA is the correction term in db for signal attenuation and g' is the mean gradient value (0 - 1000m). In equation 62, N is the surface coindex value. Some authors prefer a factor of 0.4 or 0.3 in equation 61, instead of 0.5. Further applications of equations 61 and 62 (in a modified form) are deferred until the next section.

10. Minimum signal levels, mean signal levels, and standard deviations may be estimated in a general way from climatic data as mentioned above in paragraph 8. On the other hand, maximal signal levels present a different problem. Maximal levels occur during the most favorable monthly periods and appear to be closely associated with stable meteorological conditions. Maximal signals are of primary concern in tropo networks where interference phenomena may occur between several different tropo terminals within the network. Also, security considerations may be important, either in military installations or in peace-time installations, where significant radiated signal levels may penetrate a sovereign national boundary. In general, large signal level increases tend to occur from increased magnitudes of reflection signals as well as from ducting, super-refraction phenomena, etc.

a. It should be noted that sub-refraction can sometimes occur,

which will cause refraction away from instead of toward the earth's surface. This phenomena can reduce signal levels significantly. Also, the formation of elevated ducts can result in a significant reduction of received signal levels at a particular receiver terminal. In such a situation, the elevated duct may effectively "capture" transmitted energy and drastically reduce the scattered and/or reflected energy present at the receiver. In such environments, it is believed that experimental data from a trial tropo link constitute the only principal source of information as to whether successful communications can be maintained. (In such cases it is assumed that the tropo path length is sufficiently large such that the deep fades resulting from sub-refraction and/or duct trapping cannot be tolerated, i.e., received signal levels will be below acceptable levels for a significant percentage of the time).

b. For a quantitative prediction of maximal signal levels on a given tropo link, locally obtained refractive index values (including an established empirical relationship between attenuation and index values) or representative data on received signal levels are considered as a requirement. On the other hand, a qualitative prediction can be obtained from the characteristics of the climatic environment.

c. Over-water tropo paths may also be subject to frequent duct formations, particularly in tropical and subtropical environments. Again, the need for representative data in any given situation is evident and considered as a requirement.

d. Maximal signal levels have been studied to some extent for temperate climates. An example is shown in Figure 10. These results were obtained from a collection of data by a joint American and European study

FIGURE 10

MAXIMAL FIELD STRENGTHS

1%, 10%, 50% of Time

(1kW Transmitter
450 mHz ≤ f ≤ 1000 mHz)

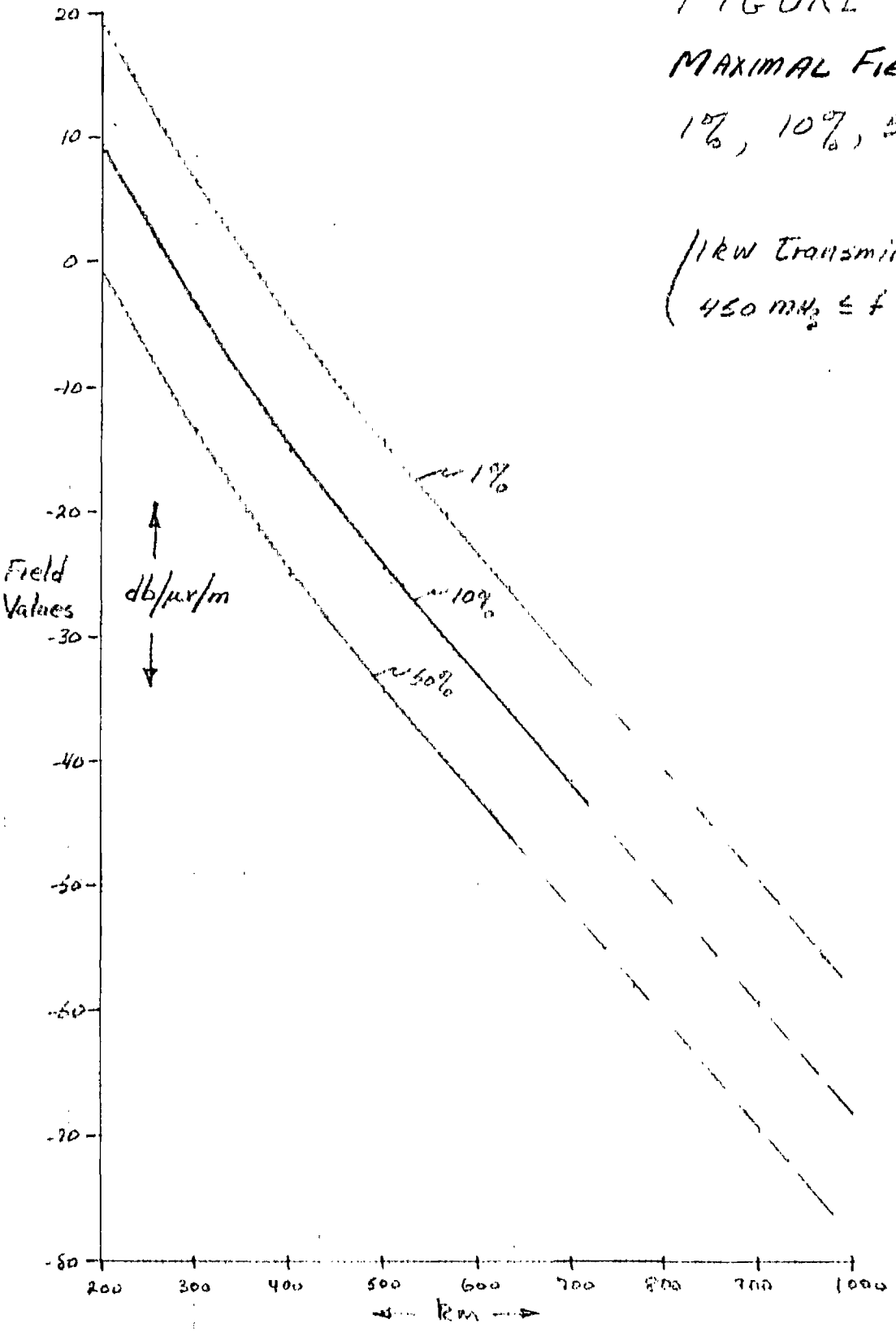

group.[32] As indicated in the figure, maximum levels which may not be exceeded for 1% of the time are approximately 20 db higher than the median (50%) value. However, significantly larger maximum levels may occur, for instance, in some tropical environments. Measurements in Senegal (French territory on the west coast of Africa) indicate possible increases of 40 db between the 50% and 1% values of mean signals (Reference 9, Figure III 12).

11. The effects of operating frequency on received tropo signals is not resolved at the present time. Some authors have established empirical relationships which indicate no frequency dependence (other than the free space dependence of f^{-2}) and specify appropriate usage of the relationships over the band from 300 to 3000 MHz. Other authors prefer a frequency dependence factor equivalent to f^{-1} or f^{-2}. As has been mentioned, a frequency dependence of f^{-1} (or λ) results from scattering theory and a frequency dependence of f^{-2} (or λ^2) results from diffuse reflection theory. Still other authors prefer a modified frequency factor. The latter usage has been adapted for this study (Reference 9, Chart P10). A plot of the frequency correction term relative to 900 MHz is shown in Figure 11.

12. The effects of antenna elevation angles have also been studied. Experimental results obtained by Svien[20] are sketched in Figure 12. In general, the additional signal attenuation which can occur due to positive elevation angles appears to be approximately proportioned to θ^3. However, for a given sum of the transmitter and receiver positive elevation angles, signal attenuations increase significantly for path distances less than 300 to 400 km. The plot in Figure 12 also indicates the approximate advantages to be gained with use of negative elevation angles. The values shown are in approximate agreement with other experimentally obtained values.

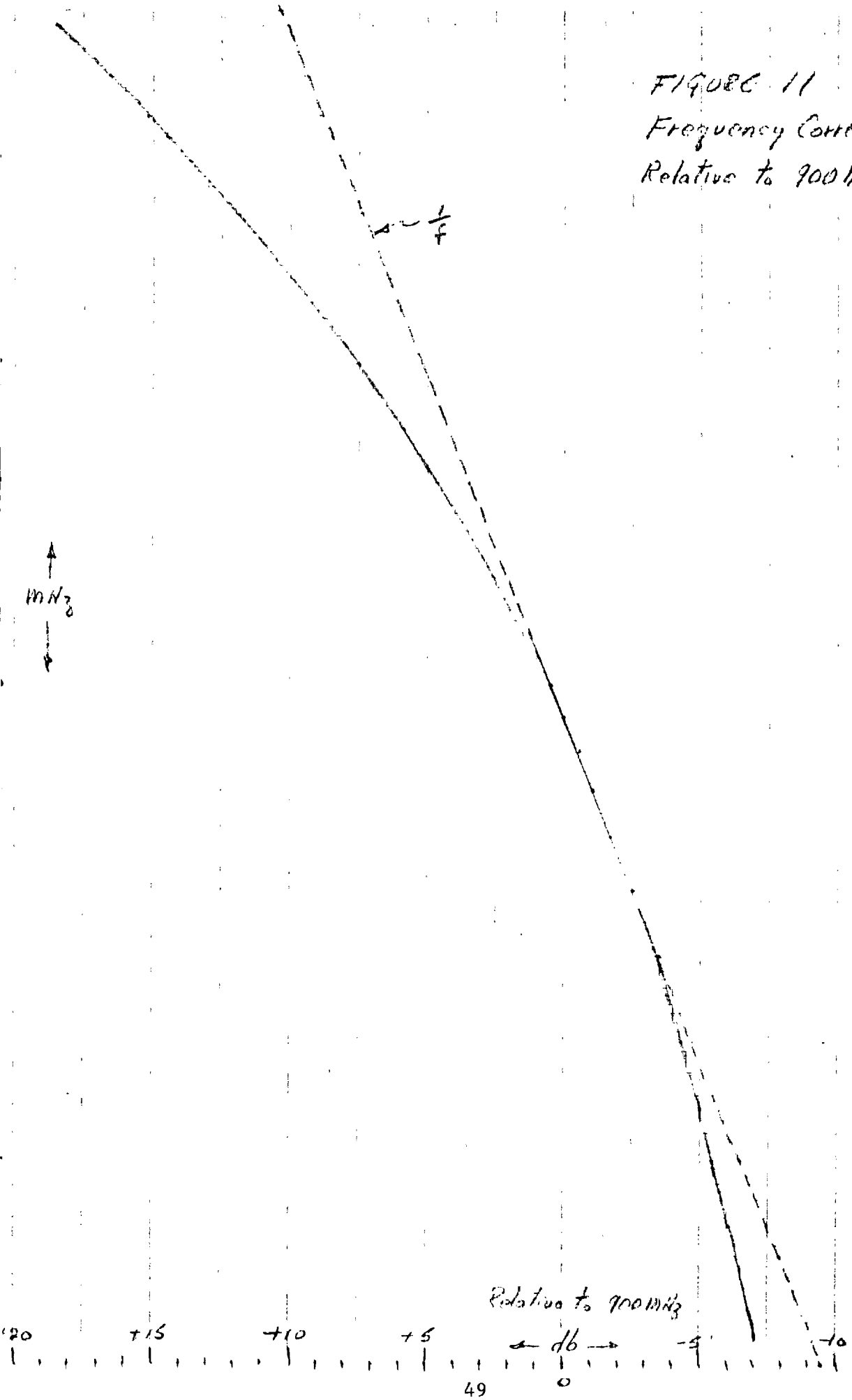
FIGURE 11
Frequency Correction
Relative to 900 MHz
$\Delta \sim \frac{1}{f}$
MHz
Relative to 900 MHz
+20
+15
+10
+5
db
-5
-10
0

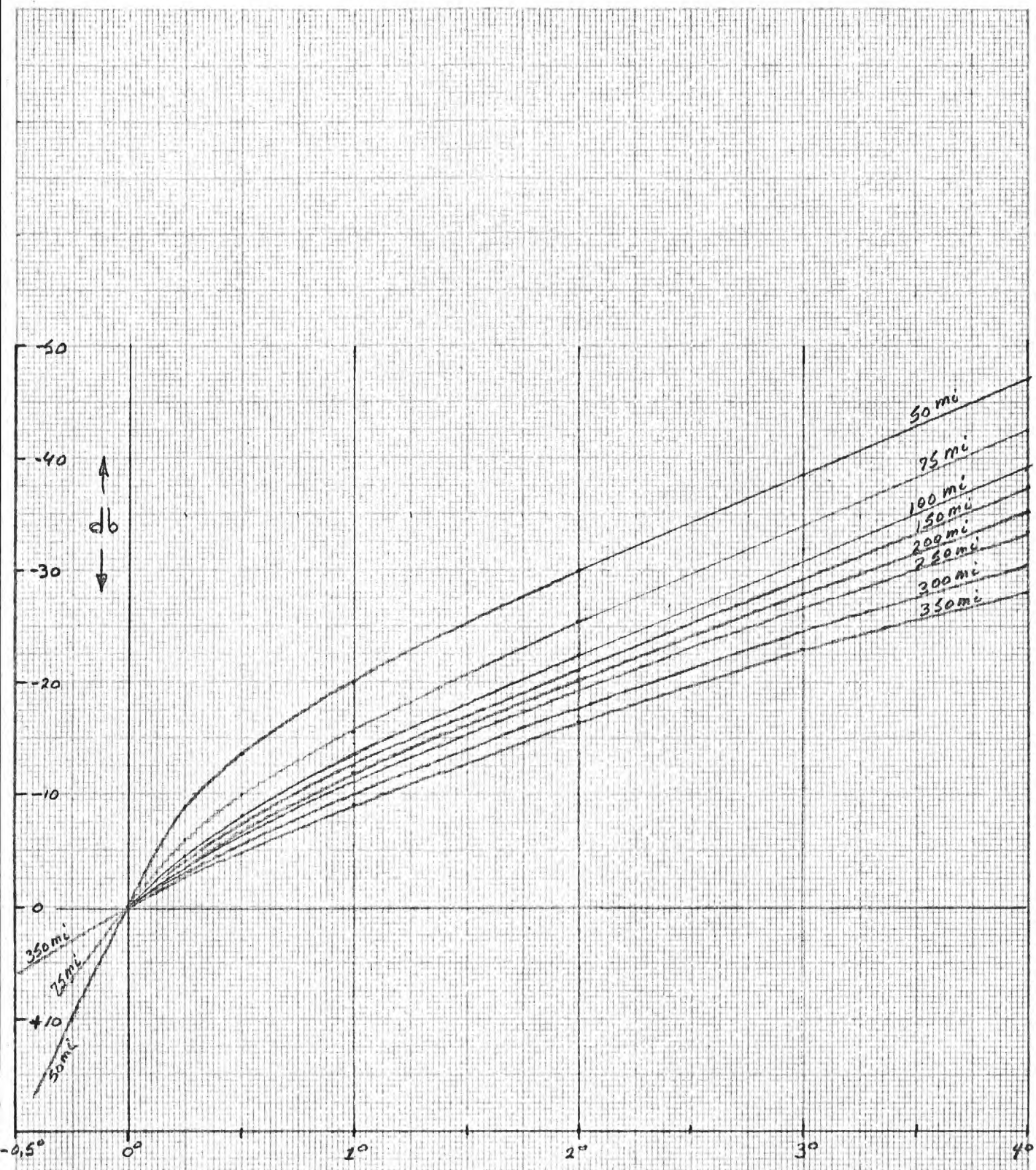

SUM OF HORIZON ANGLES
(Reference 23)

FIGURE 12

Antenna Elevation Angle Effects

13. The effects of antenna-to-medium coupling have also been studied. Such effects generally relate to the antenna beam width as compared to the total common volume for a particular path. For instance, it is possible to utilize an antenna beam width which is sufficiently small, such that the total common volume is limited by antenna beam width and not by the existent geographical and tropospheric conditions. Such effects have been measured and can be explained, based on scattering theory.[33,34] A sketch of the signal attenuation dependence on the ratio of the path angular distance to antenna aperture is shown in Figure 13 (Reference 9, Chart E_2). Antenna aperture is considered here as the antenna beam width at the half power points. If the beam widths are different for the transmitter and receiver antennas, the equivalent beam width, ω, may be determined as

$$\frac{2}{\omega^2} = \frac{1}{\omega_t^2} + \frac{1}{\omega_r^2} \qquad 63$$

The angular distance in Figure 13 relates to the distance between the transmitter and receiver radio horizons and may be determined as

$$\theta = \frac{d \text{ (interval between radio horizons)}}{r' \text{ (effective earth radius)}} \quad . \qquad 64$$

14. Because of the statistical nature of received tropo signals, it is usually possible to improve the net level of received signals by the utilization of space and/or frequency diversity systems. For any given tropo path, there are a large number of discrete paths by which RF energy can be scattered and/or reflected to a receiving antenna. Different discrete paths will evidence different received signal characteristics, both with respect to amplitude and phase. At a given receiver terminal, these many

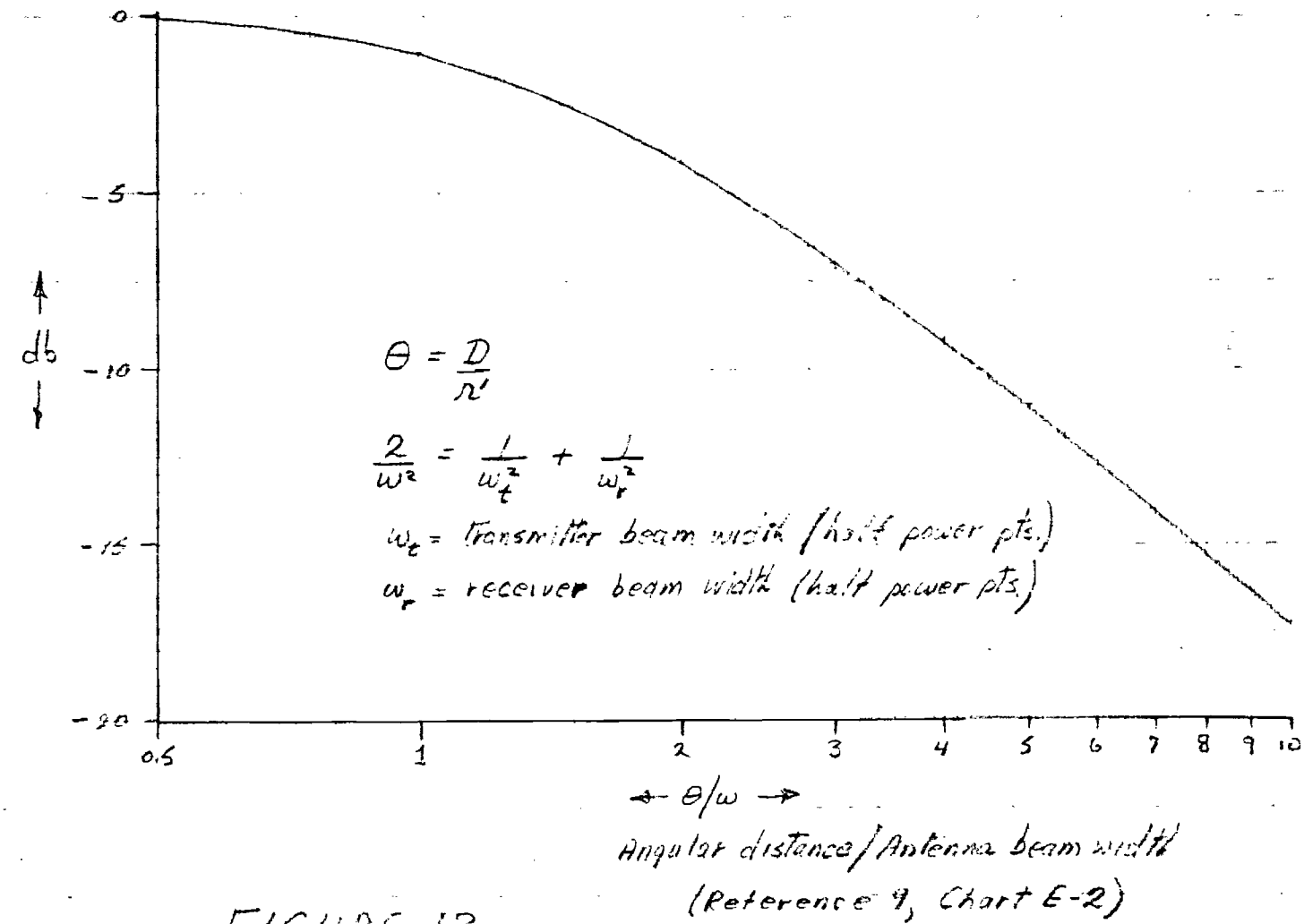

FIGURE 13

ANTENNA TO MEDIUM COUPLING LOSS

different signals constitute the total instantaneous received signal. The rapid fluctuations of the total signal can be represented as a constructive and a destructive interference phenomenon between the many discrete signals. If two physically separated receiver antennas are utilized at a given receiver terminal, the rapid signal fluctuations at one antenna site will not be identical to those at the second antenna site. That is, the signal at one antenna does not tend to vary in phase and amplitude in the same manner and at the same time as the signal at another antenna. This characteristic of incoming signals has been labeled as space incoherence and is related to the scattering mechanism of tropo propagation. Similar effects can be obtained by utilizing two or more carrier frequencies at a transmitting terminal to convey the same communications information to a receiver terminal. Similar to the former case of space diversity, the rapid signal fluctuations at one frequency do not tend to vary in the same manner and at the same time as those at the second frequency.

a. The use of two or more spaced-apart receiver antennas (operating on the same frequency) has been labeled as a space-diversity system. Theoretical results for space diversity distances have been obtained for scattered signals and for diffuse reflected signals. Generally, the minimal distances are 25 wave lengths for vertical separations, 30 wave lengths for transverse separations, and 150 wave lengths for longitudinal separations (along the path direction). In practice, separations of 100 wave lengths for transverse or vertical separations and 500 or more wave lengths for longitudinal separations are recommended.

b. The use of two or more separate carrier frequencies for transmission of the same communications information has been labeled as a

frequency diversity system. Frequency separations of 10 MHz or more are recommended for each carrier frequency. An interesting application of frequency diversity equipment has been introduced to Motorola Inc.,[35] labeled as the AN/TRC-105 Lightweight Troposcatter equipment. The system involves a frequency sweep technique, utilizing frequency steps of 1.25 MHz, for 16 separate frequencies. For the relatively small discrete frequency separations of 1.25 MHz, a relatively high degree of correlation was expected between each signal on each adjacent frequency. However, the correlation factor between the next adjacent frequencies was theoretically calculated at less than 0.1. Therefore, if alternate frequencies were considered to produce incoherent received signals (correlation factors less than 0.1), the 8 alternate frequencies should be theoretically equivalent to an 8th order frequency diversity system. In practice, over an 80 nautical mile test link between Englin (Florida) and Brookley (Alabama) Air Force bases, approximately a 5th order frequency diversity system was realized. Thus, the net effective signal was improved by 4.5 db at the median (50%) value, 16 db at the 99% value, and 30 db at the 99.9% value.

c. When rapid signal fluctuations follow a Rayleigh distribution, the expected improvements due to utilization of diversity systems are sketched in Figure 14. Thus, significant improvements in the effective received signal levels can be realized. When the received signal fluctuations are less dispersed than a Rayleigh distribution (for instance, during stable meteorological conditions) proportionately smaller net signal improvements are expected. The degree of improvement will depend on the number of reflecting layers contributing to diffuse reflected signals and on the relative magnitudes of the diffused reflected and scattered signals (see previous Figure 8).

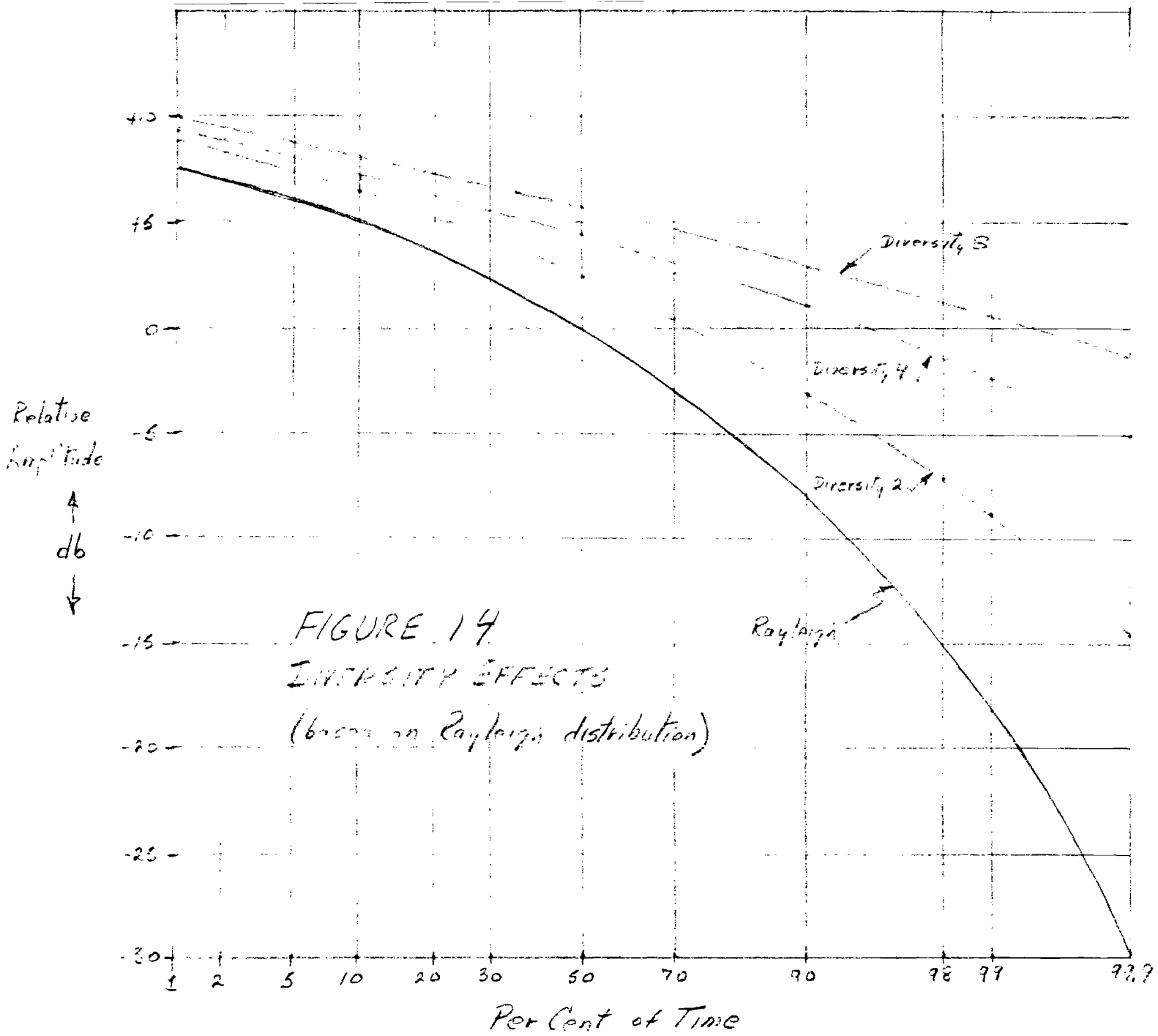

FIGURE 14
DIVERSITY EFFECTS
(based on Rayleigh distribution)

D. Empirical Relations

1. As a general approach to the varied problems of estimating received tropo signals on any given link, empirical relations are recommended at the present time. A number of different empirical relationships[19,20,21,22,23,24] have been developed and may be found in the literature. The empirical curves used in this report have been developed based on these published relationships as well as on data from a number of experimental and operational tropo links.

2. Median signal levels for any given tropo link are categorized by climatic location. These relationships are shown in Figure 15, and are similar in shape to those given in reference 9, Figure VI 6. Attenuation below free space versus total path distance is indicated for the six climates. For temperate climates, the indicated median values are from 3 to 7 db below other published curves, and are, therefore, somewhat more pessimitic. The curves of Figure 15 are representative of worst case conditions, for the most unfavorable hours during the most unfavorable months and for the most unfavorable season. The values are based on a frequency of 900 MHz and should be adjusted for other frequencies through utilization of the previous Figure 11. The transmitter and receiver antennas are assumed to be located on the earth's surface with zero elevation angles. For other elevation angles, the curves of Figure 15 should be adjusted through utilization of the previous Figure 12. If necessary, adjustments for antenna-to-medium coupling losses can be made through utilization of the curve of Figure 13. Most authors indicate that antenna height corrections are not necessary for nominal values of surface located antennas. That is, the total path distances for the curves of Figure 15 may be considered to apply between terminals. Further study will be necessary to evaluate usage of equivalent distances (instead of linear distances) and any effects of antenna elevations.

FIGURE 15
Median (50%) Signal Levels

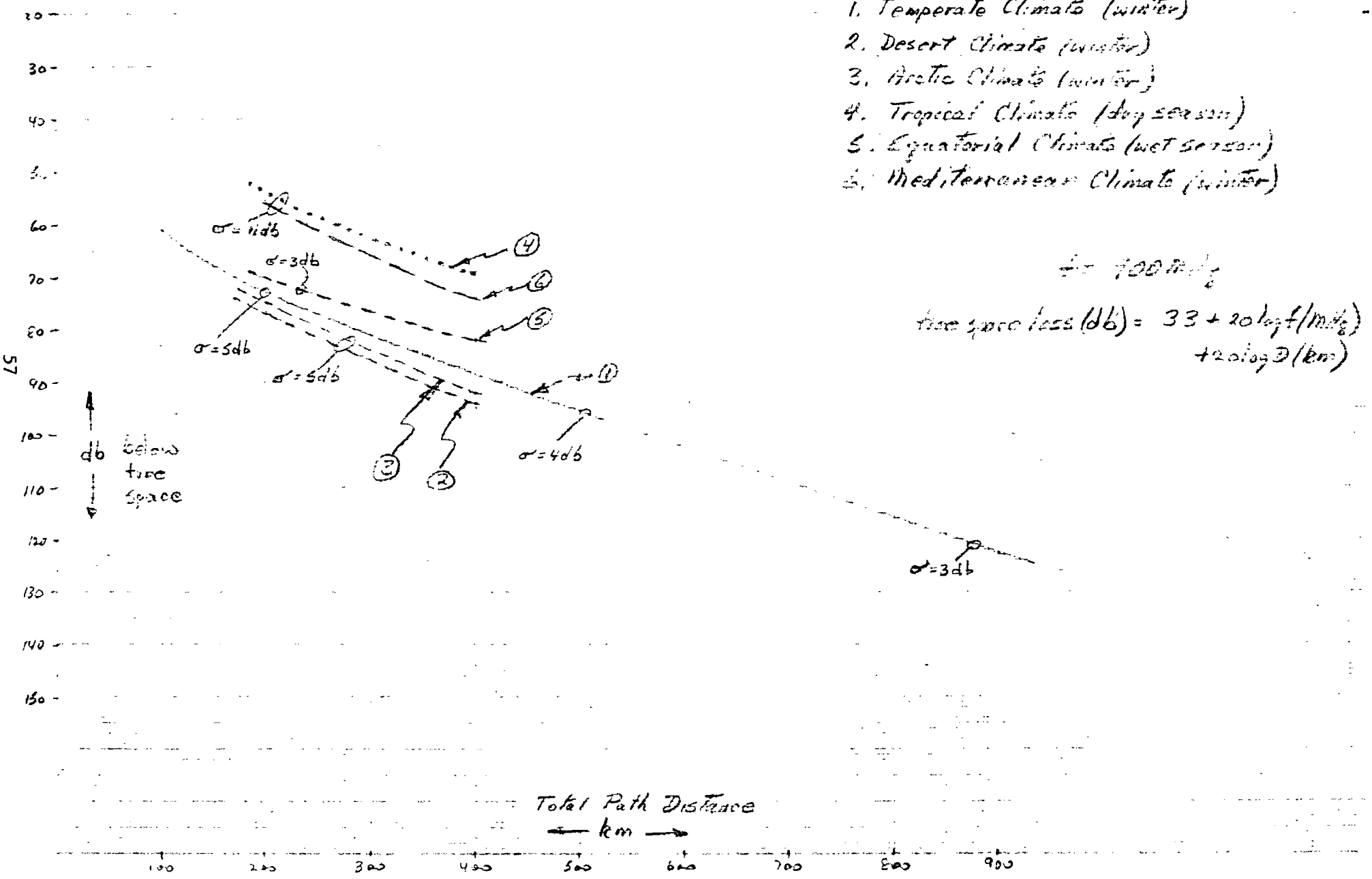

3. The mean standard deviations also are indicated for the curves of Figure 15. These may be related to computations of the corresponding mean values at 90%, 99%, and 99.9%. In Figure 16, the corresponding 99% mean values are indicated for the six climatic regions. With the exclusion of the temperate climatic curve, the remaining five curves are based on DuCastel's empirical curves (Reference 9) for 99% mean values with respect to the temperate curve.

4. For the temperate climate curves (Figure 15 and 16), further corrections may be desirable. For instance, diurnal, monthly and seasonal effects can be applied as appropriate. Mean values for these signal level changes have been indicated in a general way in the previous section, paragraph 8. More representative values for these signal changes for any given location may often be obtained through usage of attenuation correction factors as follows.

a. General attenuation corrections have been given in the previous section, paragraph 9e, through equations 61 and 62. For prediction of signal changes in the temperate climates, the following equation may be useful:

$$\Delta A = a - b(N_s - 31), \qquad 65$$

where ΔA is the attenuation correction in db, a is an adjustment constant, b is a constant dependent on path distance, and N_s is the surface value of the coindex at the particular tropo path location. For instance, in many cases the temperate curve (1) in Figure 15 may indicate excessively large attenuation values unless appropriate corrections are made for mean refractive index values. Thus, curve (1) may be considered as representative of 50% (median) signal values for temperate climates where $N_s \sim 310$. If N_s

FIGURE 16
Mean (99%) Signal Levels

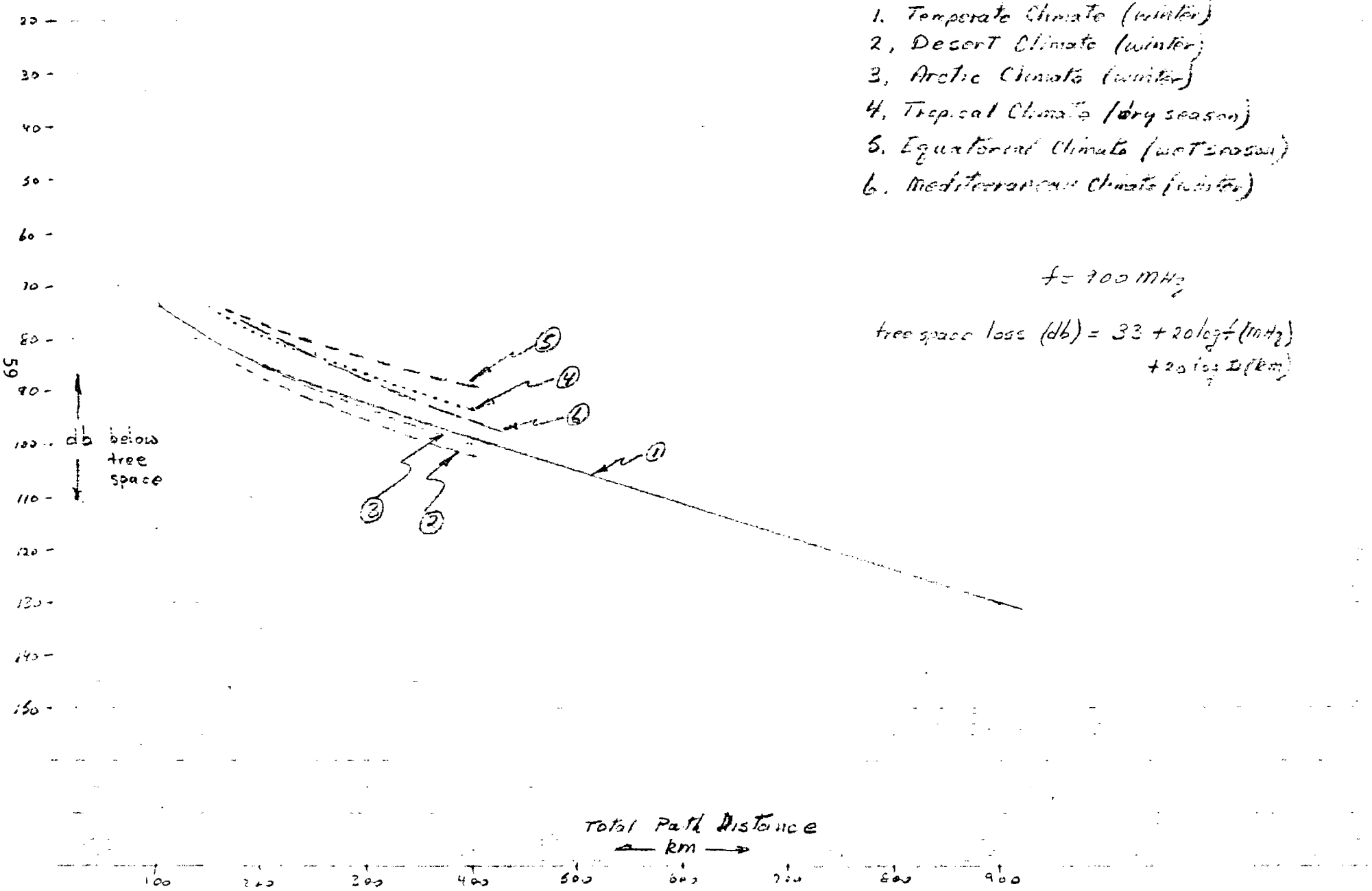

were less than 310, a larger attenuation than that indicated by curve (1) would be expected. For N_s values larger than 310, a smaller attenuation than that indicated by curve (1) would be expected.

b. As an example of the usage of equation 65, let b ~ 0.5. Then ΔA with respect to N_s changes alone would be

$$\Delta A_1 = - 0.5(N_s - 310). \qquad 66$$

For N_s changes along the northeastern New Jersey coast, $N_s \sim 315$ in February and $N_s \sim 360$ in August; $\Delta A \sim 45$. Therefore,

$$\Delta A_1 = - 0.5 \ [N \ (Aug) - 310] - [N_s (Feb) - 310] \ ,$$

$$\Delta A_1 = - 0.5 \left[(360-310) - (315 - 310)\right] \ ,$$

$$\Delta A_1 = - 22.5 \text{ db}. \qquad 67$$

The value of - 22.5 db in equation 67 is representative of a measured seasonal variation for this temperate region; i.e., measured value of - 26 db.[36] (It should be noted that this seasonal value for a temperate climate is larger than the mean value of 15 db given in the previous section C, paragraph 8.)

c. In equation 65, the value of a may be used to adjust the scale factor for maximum expected attenuations. In the case cited above for the New Jersey coast, the median value for December (worst month) was about 92 db/free space for a 300 km path at 3700 MHz. From Curve (1) Figure 15, 81 db/fs is obtained for a path distance of 300 km. After a frequency correction of + 9 db (Figure 11), a value of 90 db/fs is obtained. Therefore, for this case (using equation 65),

$$\Delta A = a - 0.5\,[N_s(\text{winter}) - 310],$$

$$\Delta A = a - 0.5\,[315 - 310],$$

$$\Delta A = a - 2.5 \text{ db}.$$

From the above predicted value of 90 db/fs and the measured value of 92 db/fs, it would appear that ΔA should be +2 db, and, consequently, a = +5 db. This assumes for the New Jersey link that approximately zero elevation angles were utilized.

d. For other values measured at 420 MHz along the northeastern coast[5] of the United States (previous Figure 9), the hourly median values were

(1) 150 km - 56 db/fs + 3 db(freq. con.) = 59 db/fs,

(2) 300 km - 66 db/fs + 3 db(freq. con.) = 69 db/fs,

(3) 560 km - 85 db/fs + 3 db(freq. con.) = 88 db/fs,

(4) 900 km - 112 db/fs + 3 db(freq. con.) = 115 db/fs,

Corresponding empirical values from Figure 15 are

(5) 150 km - 67.5 db/fs,

(6) 300 km - 81 db/fs,

(7) 560 km - 100 db/fs,

(8) 900 km - 123 db/fs.

For these data, a = -5 db would appear to be a more reasonable value. (The actual values of N_s over the region were not published and $N_s \sim 315$ has been assumed.)

5. Similar applications can be made for other climatic regions, if appropriate constant values for a and b are assumed. For instance, for a 310 km tropo path located in the region of Fort Trinquet (Sahara, Africa),

an attenuation of about 79 db/fs was measured[37] at 450 MHz. After the appropriate frequency correction (Figure 11), the signal level would be 83 db/fs, as compared to 87 db/fs from curve 2, Figure 15. For this region, g values range from about -23N units/km (winter) to -35N units/km (summer). The seasonal change is about 8 db.

If a mean value of g = -23N units/km is used at the "standard" index gradient for this desert region during winter months, (instead of the value of 40 given in equation 61 of the previous section), then

$$\Delta A = a + 0.6(g + 23), \qquad 69$$

$$\Delta A \text{ (winter)} = a + .6(-23 + 23),$$

$$\Delta A = a.$$

Therefore, a = -4 db, in order to bring predicted values (87 db/fs) from curve 2, Figure 15, into agreement with experimental values (83 db/fs). Then,

$$\Delta A \text{ (seasonal)} = 0.6(-35 + 23),$$

$$\Delta A \text{ (seasonal)} = -7.2 \text{ db}.$$

The seasonal change of ~7 db less attenuation is in approximate agreement with a mean seasonal change of 8 db.

6. For a tropical path of 270 km at Dakar (Senegal), a median level of about 51 db/fs was obtained during the dry season[37] at 430 MHz. From curve 4, Figure 15, a corresponding value of 60 db/fs is obtained. After a -3 db correction for frequency is applied, a predicted value of 57 db/fs is obtained and is to be compared with the measured value of 51 db/fs. If mean gradient values are to be utilized, the following equation for attenuation correction values might be utilized instead of equation 68 above, (or instead of equation 61 of the previous section),

$$\Delta A = a + b\,[g - g\ (\text{winter season})]. \qquad 70$$

Therefore, it would appear that the value of a in equation 70 would be -6db in order to bring prediction values (57 db/fs) into agreement with measured values (51 db/fs). Also, the mean g values appear to range from -64 N units/km (dry season) to -90 N units/km (wet season). Hence, equation 70 might be rewritten for this case as

$$\Delta A = -6 + .6(g + 64).$$

Then,

$$\Delta A\ (\text{seasonal}) = .6(-90 + 64),$$

$$\Delta A\ (\text{seasonal}) = -16\ \text{db}.$$

If equation 68 had been utilized to predict ΔA (seasonal), a value of -17.5 db would have been obtained since N_s (dry season) ~325 and N_s (wet season) ~360.

7. When attenuation corrections are applied to the curves of Figure 15, through the use of equations of the same form as equations 68 and 70, the appropriate values of the constants, a and b, should be adjudged from previously collected data from the geographical region in question.

8. Predicted values of the standard deviation may be assessed from the previous Figures 7 and 8. Under predominantly scattering conditions, the Rayleigh distribution of Figure 7 may be used. When a mixture of turbulent and stable layers exist, estimates based on the curves of Figure 8 may be made. Predicted signal level improvements by the use of diversity systems may be ascertained from the curves of Figure 14. It is noted that these latter curves are based on a Rayleigh distribution.

9. When predominantly stable conditions exist, the indicated values of the curves in Figure 15 may be increased by 10 to 15 db. In addition, the type of signal fluctuations will decrease from a Rayleigh distribution; i.e., become considerably less dispersed. However, deep fades (signal variations) of 10 to 20 db may occur due to destructive interference phenomena from the predominantly diffuse and/or specular reflected signals.

E. Diffraction Path Considerations

1. It has been mentioned that tropo signal levels may be affected by diffracted signals for path distance less than about 200 km. Therefore, for such path lengths it may be desirable to predict diffraction signal levels as well as tropo signal levels.

2. When a communication link is situated on relatively flat ground, when terminals have similar heights, and when elevation angles are near zero, the diffraction path may be taken as that path having a radius equivalent to the corrected earth radius. That is, for a standard atmosphere, the diffraction path with a radius equal to 4/3 of the real earth radius would be used. For a non-standard atmosphere, the appropriate equivalent radius would be used. The curves shown in Figure 17 may be utilized to obtain a corrected distance value, d_o, dependent on frequency and equivalent radius. Subsequently, the curves shown in Figure 18 may be utilized to obtain the predicted attenuation below free space, based on the ratio d/d_o.

3. Corrections for antenna heights can be obtained as follows. If the earth's surface is flat or "gently rolling" (perhaps with depressions of 50 meters or less) between the antenna and the horizon, the effective antenna height can be taken as the real antenna height, and no further attenuation correction is necessary. On the other hand, if the foreground (between antenna and horizon) is significantly depressed, either due to topography or to an elevated antenna location (perhaps 100 meters or more), an effective antenna height should be utilized. This value of effective height, h_e, may be taken as equal to the value, y, of the earth's depression for the distance between the antenna and the horizon. Equation 25, Section A,

$d_0 = \left(\frac{\lambda a'^2}{\pi}\right)^{\frac{1}{3}}$ (km)

FIGURE 17

DIFFRACTION PATHS

Corrected Distance

(Reference ?, Chart P-2)

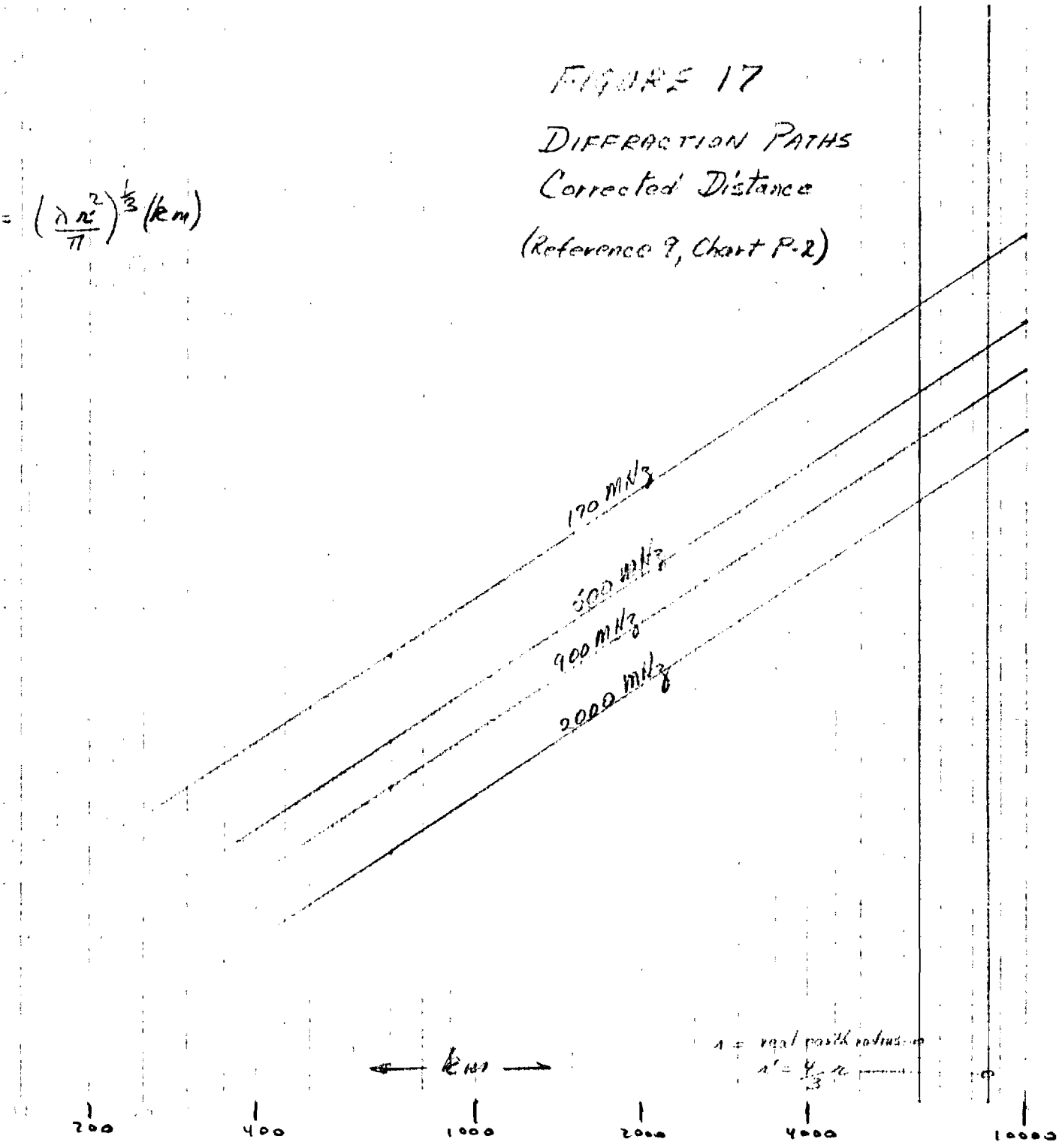

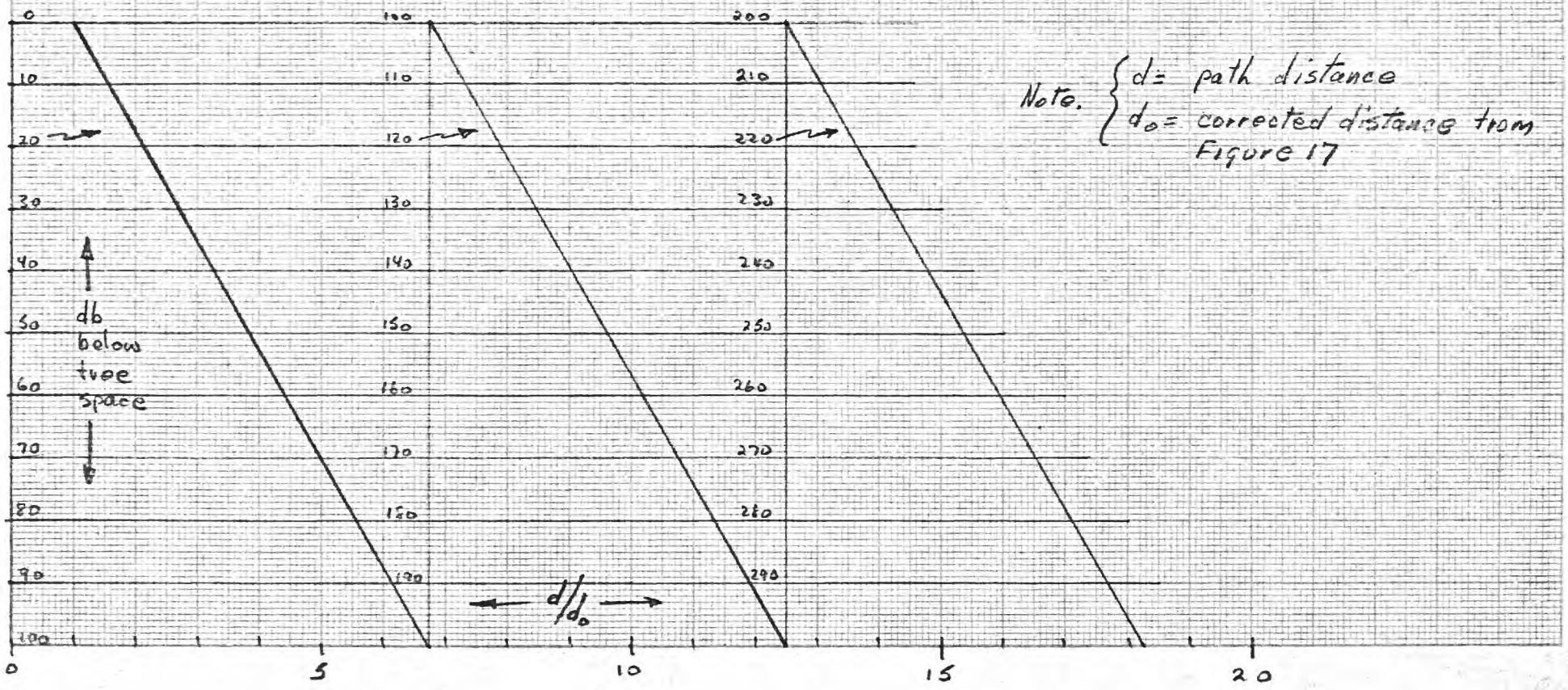

FIGURE 18

DIFFRACTION PATHS

MEAN DECIBEL LOSS

(Reference 9, Chart P-4)

Note. { d = path distance
d_o = corrected distance from Figure 17

can be used to supply the appropriate value of $y = h_e$. Dependent on the value of r' and the operating frequency, f, a normalized height value, h_o, may be determined from the curves of Figure 19. Subsequently, the additional attenuation correction associated with antenna height may be obtained from the curves of Figure 20, based on the ratio h_e/h_o.

4. Often, the topography of a link may be such that these assumptions (above paragraphs 2 and 3) are not applicable. This may occur over rough terrain with significant elevation changes and, perhaps, increased elevation angles at one or both terminals. In such situations one of several different procedures may be applicable.

a. The earth's surface may be represented by a parabolic plot, utilizing equation 25, Section A. The value of r' utilized should be equivalent to the lowest monthly mean gradient value for the link in question . Then the path profile is plotted. In particular, five elevation points are of interest.

(1) The transmitter elevation,

(2) The transmitter horizon elevation,

(3) The highest elevation between the terminal horizons,

(4) The receiver horizon elevation,

(5) The receiver elevation.

b. A parabola representing the diffraction path may be fitted to three elevation points (2), (3), and (4), listed above in subparagraph a. An example is shown in Figure 21. A standard atmosphere is assumed together with an operating frequency of 170 MHz. Therefore, the smooth earth's surface is represented by the parabola $y = (0.0585 \times 10^{-3})\, x^2$, plotted with respect to the xy coordinate system (y is measured in meters and x is measured in kilometers). The five elevation points mentioned above are listed as

$h_o = \left(\frac{\lambda^2 R'}{\epsilon \pi^2}\right)^{\frac{1}{3}}$ (meters)

FIGURE 19
DIFFRACTION PATHS
CORRECTED HEIGHT
(Reference 9, Chart P-3)

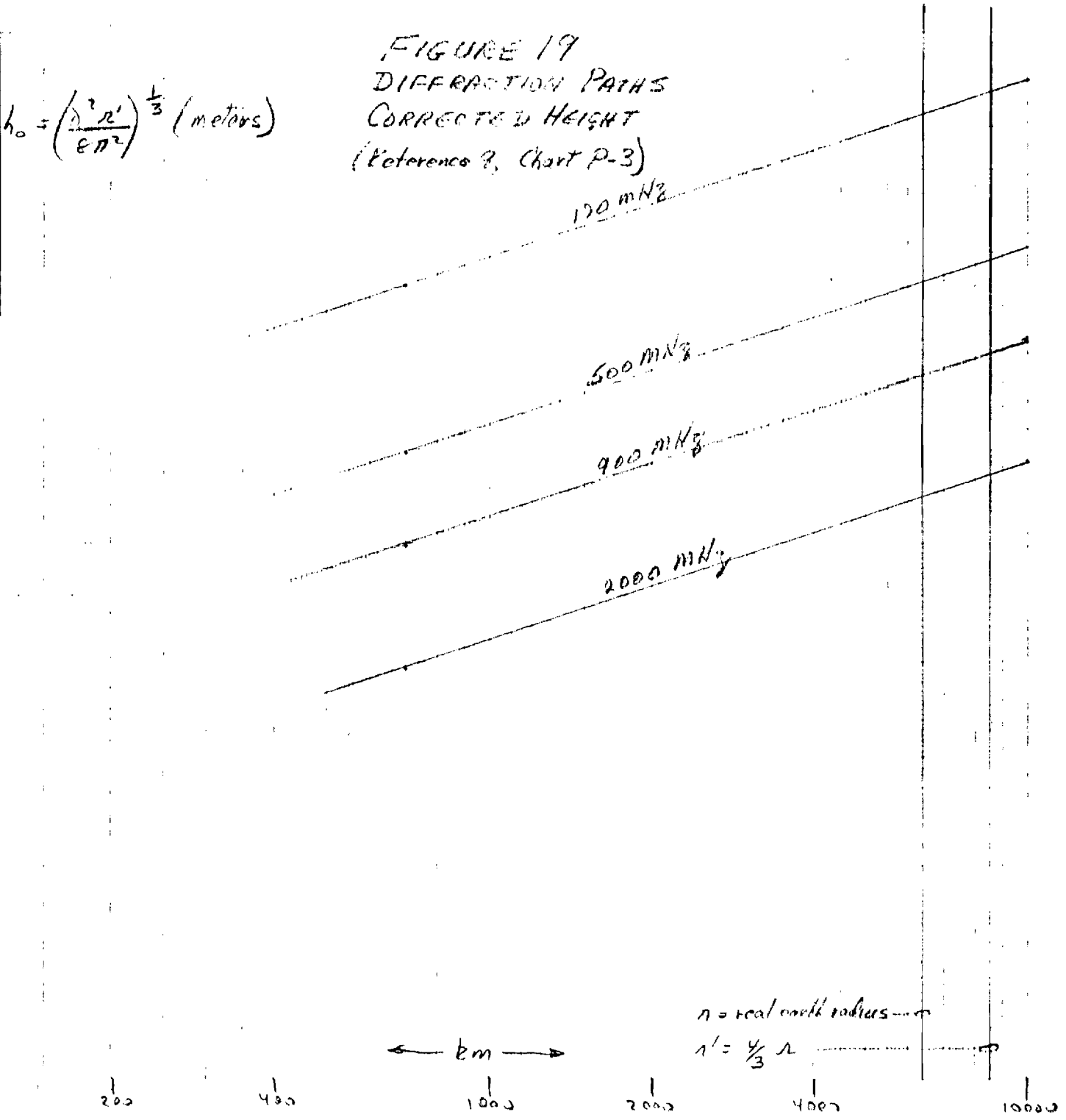

Equivalent Radius

FIGURE 20

DIFFRACTION PATHS

HEIGHT-GAIN CORRECTIONS

(Reference 9, Chart P-5)

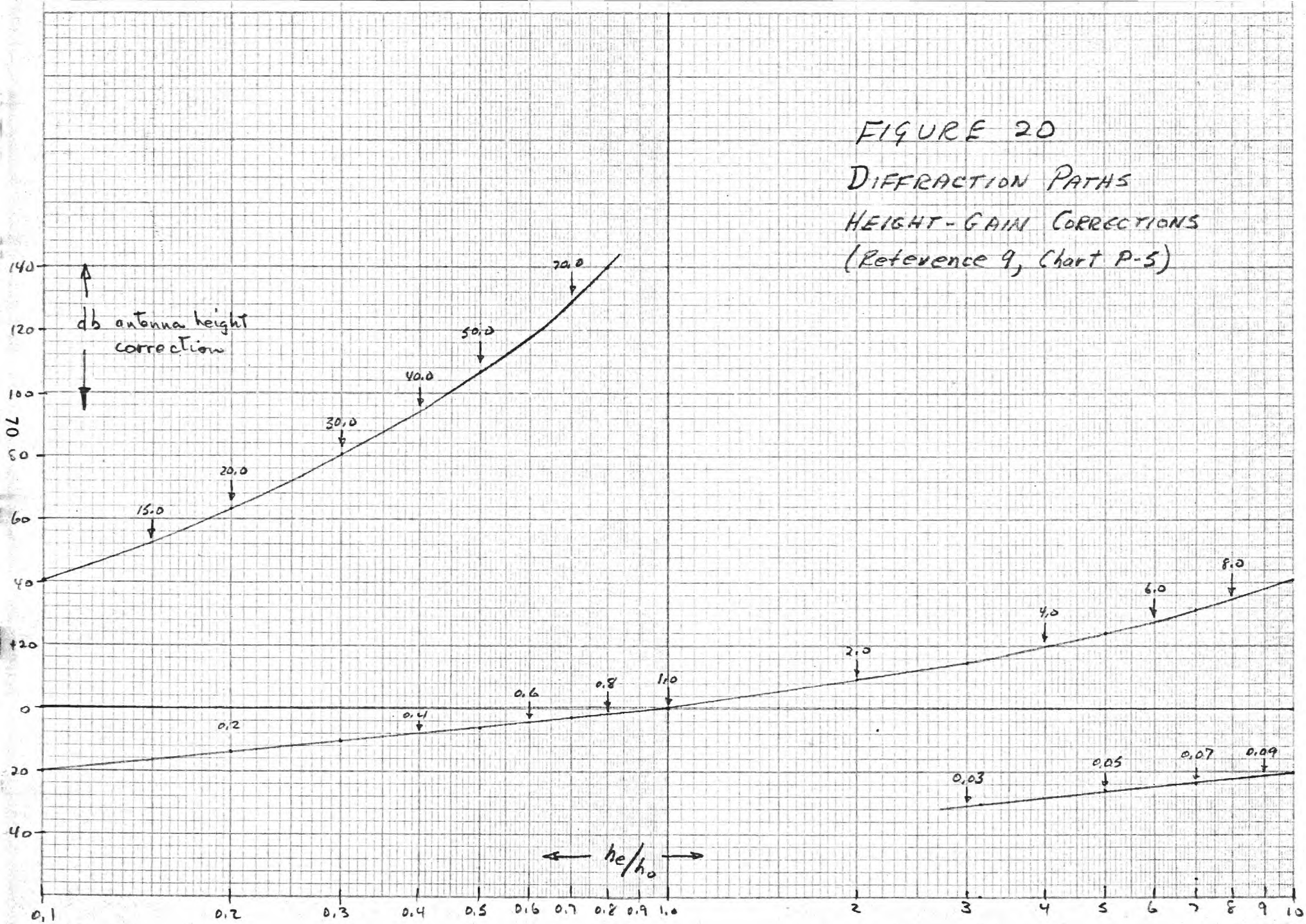

FIGURE 21
DIFFRACTION PATH
(Example 1)

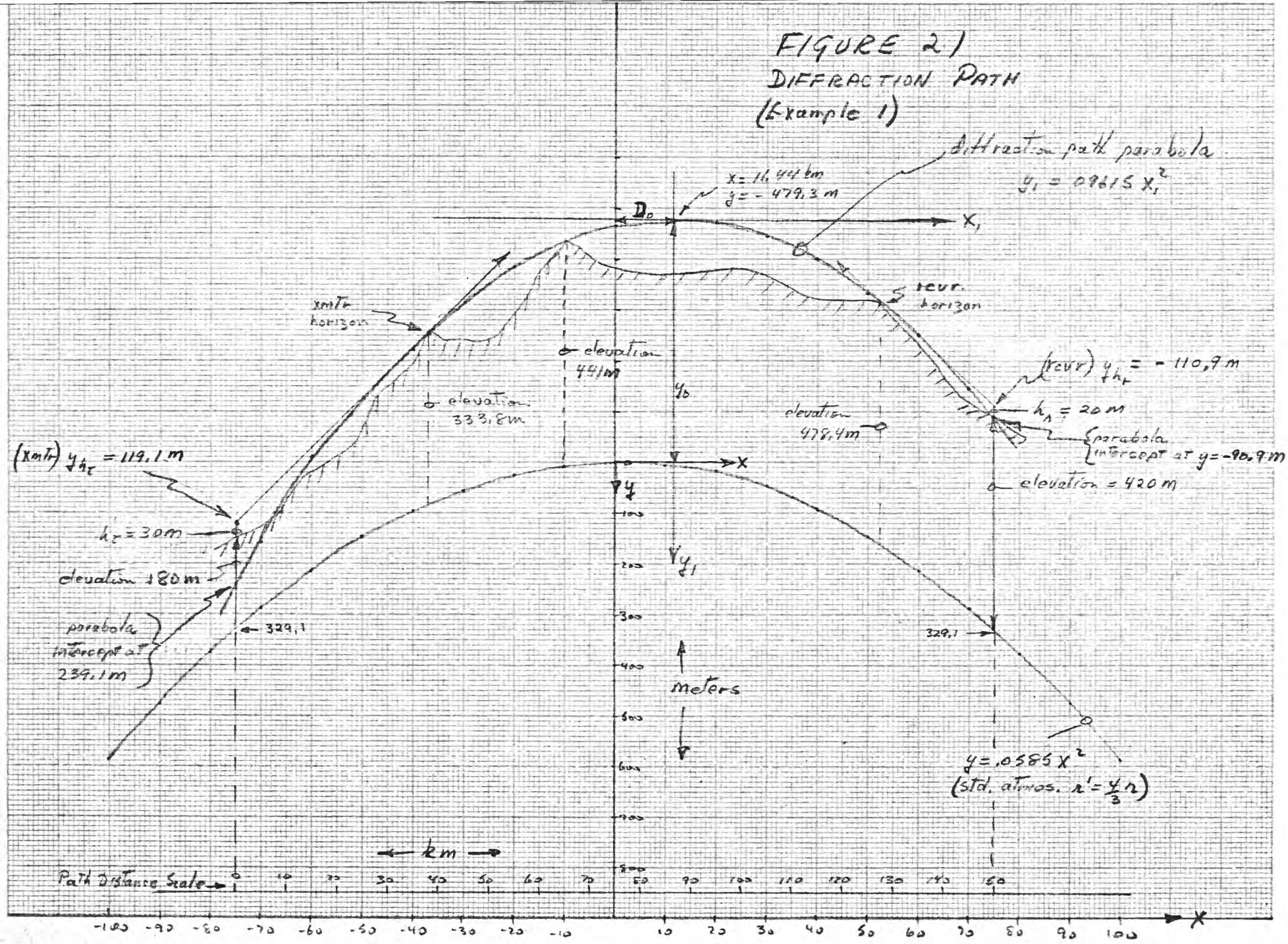

(1) transmitter, y = 119.1 m, x = -75 km

(2) transmitter horizon, y = -253.7 m, x = -37 km

(3) highest point, y = -435.1 m, x = -10 km

(4) receiver horizon, y = -317.2 m, x = 52.5 km

(5) receiver, y = -110.9 m, x = 75 km

For parabola fitting to points (2), (3), and (4) above, the following procedure can be utilized. In general,

$$y_1 = k_p x_1^2 \qquad 72$$

where $k_p = 1/2r'_p$, with respect to the xy, coordinate system. (The subscript "p" refers to path. It is noted that $r'_p \neq r'$, in general, since r' relates to the mean value of the index gradient, g. In equation 72,

$$\begin{aligned} y_1 &= (y_i - y_o) \\ x_1 &= (x_i - D_o) \end{aligned} \qquad 73$$

where D_o and y_o represent the translation of the x_1 y_1 coordinate system from the xy coordinate system. The x_i,y_i values are, respectively, the path distance and elevation for the three points (2), (3), and (4). Therefore

$$\begin{aligned} (-253.7 - y_o) &= k_p(-37-D_o)^2 \\ (-435.1 - y_o) &= k_p(-10-D_o)^2 \\ (-317.2 - y_o) &= k_p(52.5-D_o)^2 \end{aligned} \qquad 74$$

Simultaneous solution of equation 74, yields the following values for y_o and D_o,

$$y_o = -479.3 \text{ m}$$

$$D_o = 11.44 \text{ km} \qquad 75$$

From these values, k_p may be determined from equation 74 as ,

$$k_p = 0.09615 \times 10^{-3}/_{km} = 1/2r'_p, \qquad 76$$

or

$$r'_p \cong 5200 \text{ km}. \qquad 77$$

Therefore, the parabola representing the diffraction path of Figure 21 is

$$y_1 = 0.09615\ x_1^2, \qquad 78$$

where y_1 is measured in meters and x_1 is measured in kilometers.

c. The parabola of equation 78 intercepts the transmitter vertical axis at y = 239.1 m. Thus, the transmitter effective height, h_{e_t} is the difference between actual height and the value of this intercept; i.e. h_{e_t} = 239.1 - 119.1 = 120 m. The path parabola (equation 78) intercepts the receiver vertical axis at y = -90.9 m, and h_{e_r} = 110.9 - 90.9 = 10 m.

d. From Figure 17, for r'_p = 5200 km and f = 170 MHz, d_o = 25.0 km and d/d_o = 150/25.0 = 6.0. From Figure 18, for d/d_o = 6.0, the attenuation below free space is estimated as 88 db. From Figure 19, h_o = 59 m, and h_{e_t}/h_o = 120/59 = 2.0, and h_{e_r}/h_o = 10/59 = 0.17. From Figure 20, the attenuation correction for antenna heights is ΔA_t = +5 db, and ΔA_r = -15 db. Therefore, the predicted attenuation below free space for the path shown in Figure 21 is

$$A = 88 + 5 - 15 = 78 \text{ db/fs}. \qquad 79$$

5. The same link as shown in Figure 21 is reproduced in Figure 22, based on a non-standard atmpsphere. As shown, the parabolic representation of the earth utilizes a k value equal to 0.043 x 10^{-3}/km, which relates to an equivalent radius r' $\cong$ 11.6 km (g = -70 N units/km). Following the same procedures as listed paragraph 4 above, the parabola representing the diffraction path can be written as

$$y_1 = 0.0808\ x_1^2 \qquad 80$$

where y_1 is measured in meters and x_1 is measured in kilometers, with y_o = -481.7 m, and D_o = 13.6 km. The value of r_p ($= \frac{1}{2k_p}$) is 1/2(0.0808 x 10^{-3}) $\cong$ 6188 km. Also, h_{e_t} = 152.3 - 31.9 = 120.4 m, and h_{e_r} = 198.1 - 177.2 = 20.9 m, d/d_o = 150/28 = 5.4, h_{e_t}/h_o = 120.4/62.5 = 1.9, and h_{e_r}/h_o = 20.9/62.5 = 0.33. Therefore, the predicted attenuation (from Figure 18 and 20) is 77 + 9 -9 = 77 db.

6. For the two examples shown in Figures 21 and 22, there results no significant change in the predicted attenuations, However, attenuation changes of 5 to 10 db are usual for Δg changes of about $\pm$20 N units/km.

7. In Figure 21, if the maximum elevation (441 meters at x = - 10 km) has been significantly less, a smaller k_p value (less than the indicated 0.09615x10^{-3}) would have been obtained. However, the constructed path parabola must pass through or below each terminal point. Therefore, if the highest elevation point is not a determining factor in establishing the path parabola, one or the other of the terminal locations should be utilized, whichever is appropriate.

8. The desirability or necessity for including diffraction paths over common horizon obstacles has not yet been investigated. More study

FIGURE 22
DIFFRACTION PATH
(Example 2)

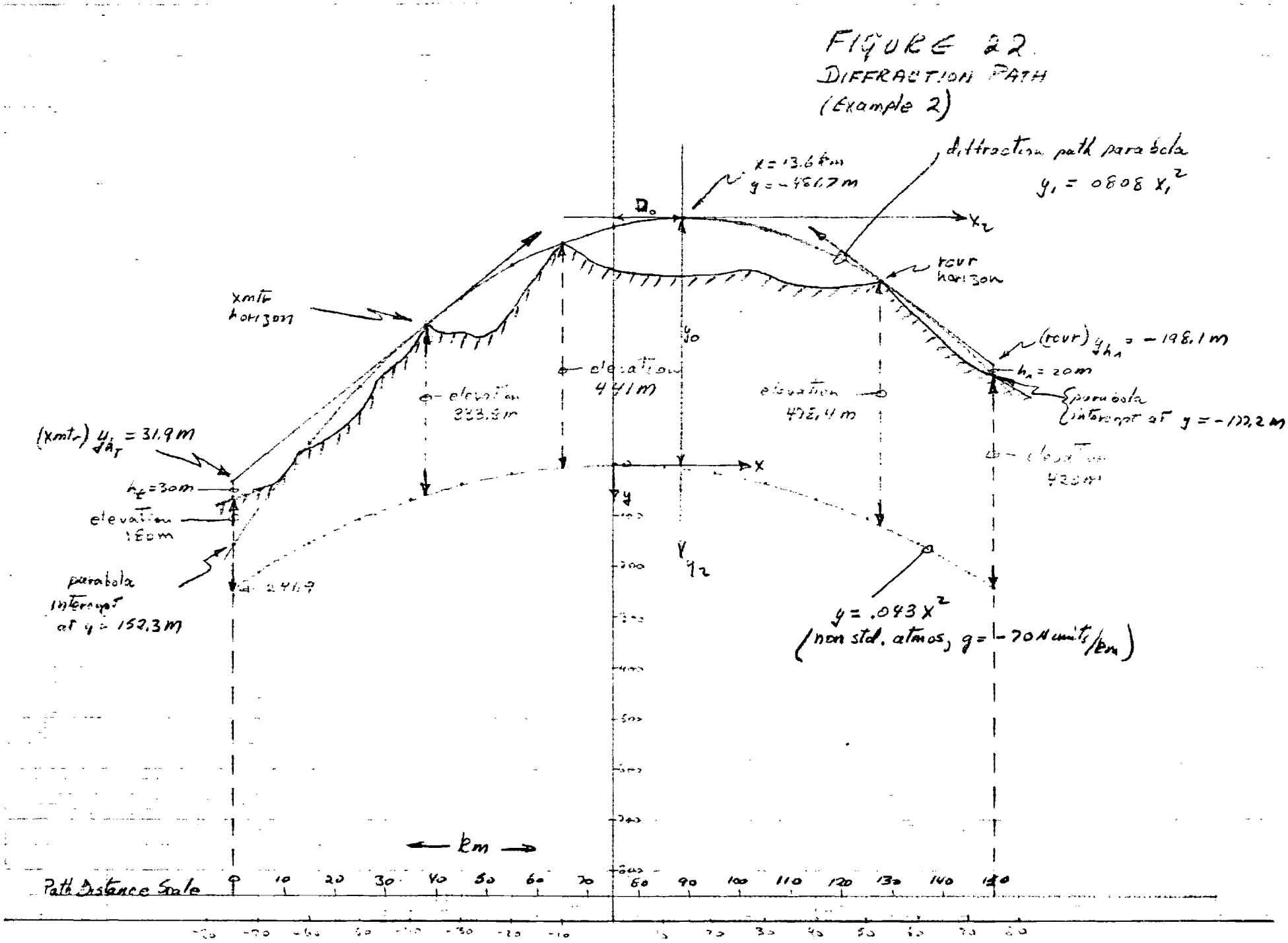

will be necessary to establish a sufficiently detailed approach which, at the same time, is general enough for wide applicability. In addition, for subsequent computer obtained solutions, the number of control parameters must be held to a minimal number for practical applications.

F. Frequency Separation Requirements and Procedures

1. When two or more troposcatter equipments are located at the same site and are operated on different links, the equipments are said to be co-sited. On a given link at a given site, one particular equipment will involve a transmitter and a receiver for the given link. Frequency separations for this transmitter and receiver are labeled as T-R (SS), where the "T" and "R" refer to transmitter and receiver, respectively, and the "SS" refers to Same System. The frequency separations between this transmitter and some other cosited receiver (involved in a different link) are labeled as T-R (DS), where the "DS" refers to Different System. In addition, at a given site, cosited transmitters and cosited receivers will have frequency separations which are labeled, respectively T-T (DS) and R-R (DS). Finally, there may exist certain "forbidden frequencies." These relate to certain isolated frequency bands which are separated by a discrete frequency from the operating frequency of a transmitter; then any cosited receiver cannot be operated within the forbidden frequency band. All of the above frequency separations relate to cosited situations. All such required frequency separations are usually listed in equipment specifications by the manufacturer. Required cosite frequency separations must be maintained; otherwise, cosite interference may occur.

2. When two or more tropo links are operated within the same area, a tropo network exists. For this situation, there will exist, in general, other required frequency separations between each transmitter and each remotely located receiver within the network. These frequency separations are necessary in order to prevent off-site interference between any transmitter and any remotely located receiver operating on a different link.

3. It is possible to maintain adequate frequency separations (between assigned frequencies) in any given tropo-network. At the same time, it is also possible to assign frequencies in a tropo network and maintain efficient utilization of these frequencies within the allotted frequency band. The principles involved have been applied successfully to radio relay networks[38] and the recommended tropo frequency management procedures of this report derive from these principles.

4. As mentioned previously, the appropriate cosite frequency separations may be obtained from manufacturers' specifications for the particular equipment type used in a tropo network. Appropriate off-site frequency situations can be obtained through the construction and use of a geographical frequency separation pattern. This pattern concept is unique[38] and has been developed by personnel of the Rich Electronic Computer Center of the Georgia Institute of Technology.

5. A geographical frequency separation pattern may be considered as a segmented plot of the transmitter antenna radiation pattern. It comprises expected received signal levels within the pattern, based on distance and orientation of receivers with respect to the transmitter orientation, and based on operating frequency differences between the transmitter and any remote receiver. For the purposes of this report, it is assumed that one particular tropo equipment type is utilized throughout the network. (Modificiations and procedures for handling different equipment types within the same geographical area can be accomplished, but are beyond the scope of this report).

6. From manufacturers' specifications (or from spectrum signature data), characteristic plots of signal level versus frequency separation (ΔF)

can be made. An example is shown in Figure 23 for AN/TRC-90 B type equipment. These curves relate to cosite situations. Two situations exist between cosited transmitters and receivers:

a. For a given transmitter there is an associated receiver (same system), both of which operate on the same link. Curve 1, Figure 23, represents the predicted signal levels in such a receiver operating on a frequency $f \pm \Delta f$. If the receiver is operated at the same frequency as the transmitter ($\Delta f = 0$), a 125dbw level is indicated. As the receiver frequency is changed ($\Delta f \neq 0$), the predicted signal level decreases to the receiver sensitivity level at $\Delta f \cong 110$ MHz. This value is the required T-R (SS) frequency separation between a transmitter and its associated receiver. In addition, there is a forbidden frequency band indicated at $f = \pm$ (140 MHz $\pm$ 5 MHz). With respect to the transmitter frequency f, the associated receiver can be operated on any frequency $f \gtrsim 100$ MHz except where $f = \pm$ (140 MHz $\pm$ 5 MHz).

b. In general, there will be other cosited transmitters and receivers. For one of these cosited receivers, the receiver antenna may be located within the main lobe of the transmitter mentioned above in a. In addition, the main lobe of this receiver antenna could be oriented toward the above mentioned transmitter. In such a situation, curve 1, Figure 23, would be applicable also as T-R (DS) for this arrangement. Therefore, curve 1 also has been labeled in Figure 23 as "major to major lobe orientation." It should be noted that this situation is most unlikely to occur, and represents a very poor site-engineering practice.

c. One of the cosited receivers might also be located within the main lobe of the above mentioned transmitter, the receiver antenna being oriented such that its minor lobe was oriented toward the transmitter.

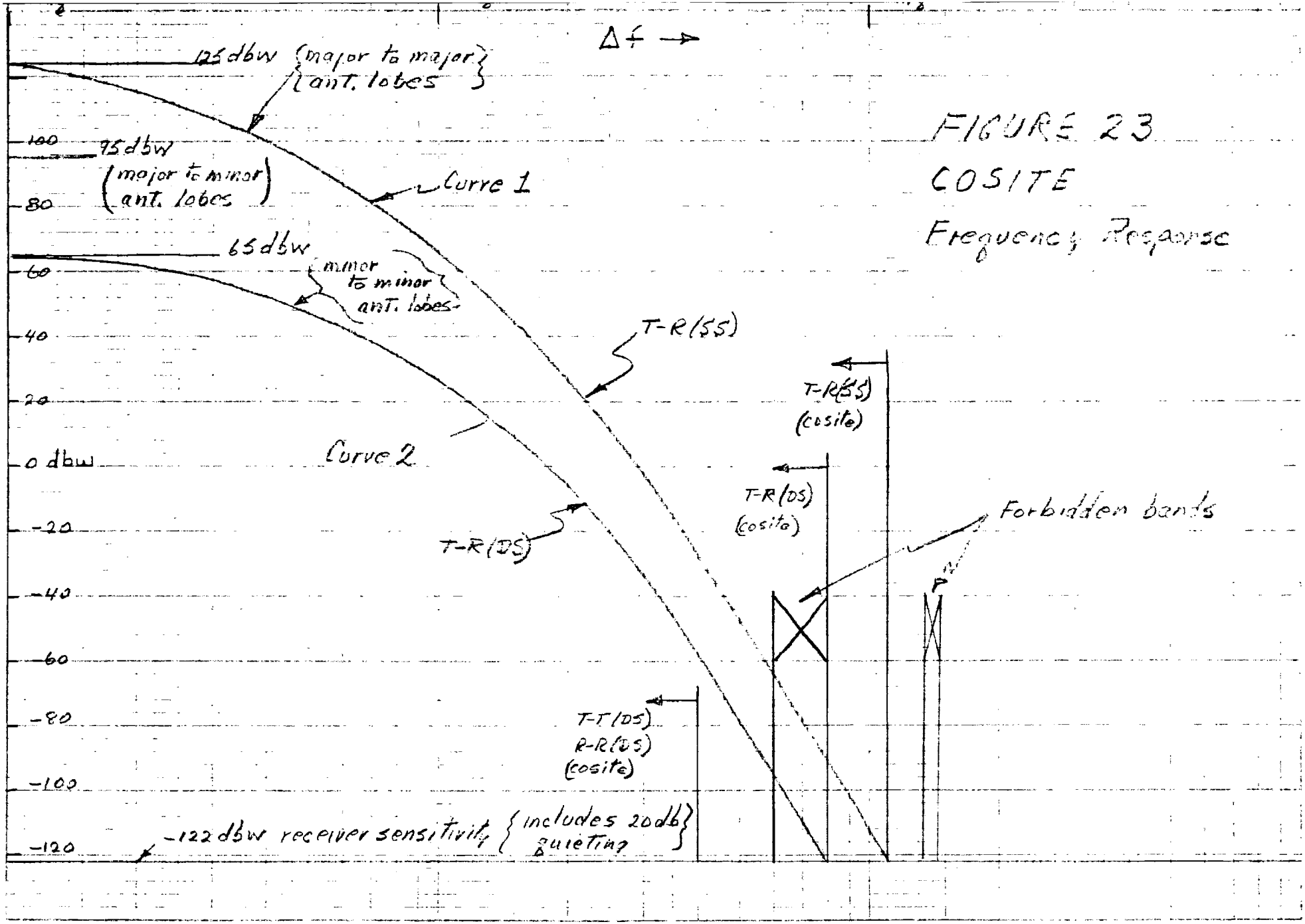

FIGURE 23

COSITE

Frequency Response

The indicated signal level for this circumstance is 95 dbw. This situation also represents a poor site-engineering practice; the corresponding frequency response curve has not been indicated in the figure.

d. The usual case for cosited receivers is indicated by Curve 2, Figure 23. In this situation, the receiver antenna is not located in the main lobe of any cosited transmitter, and the receiver antenna is not oriented toward any cosited transmitter antenna. Hence Curve 2 is labeled as T-R (DS) and represents a "minor-to-minor lobe orientation." If the operating frequency of the cosited receiver is the same as the above mentioned transmitter, a predicted signal level of 65 dbw is indicated. As the cosited receiver frequency is changed ($\Delta f \neq 0$), the predicted signal level decreases to the receiver sensitivity level at $\Delta f = 80$ MHz. In addition, required frequency separations between cosited transmitters, T-T(DS), and between cosited receivers, R-R(DS), are indicated. A forbidden frequency band is also shown. Thus T-T(DS) or R-R(DS) must be greater than 40 MHz and not equal to 70 MHz $\pm$ 10 MHz.

7. A similar type of plot for off-site conditions is shown in Figure 24. The predicted signal levels for the various antenna orientations are indicated on the ordinate scale for a distance separation of 1.6km. As the operating frequency of any given receiver is changed ($\Delta f \neq 0$), the associated signal level reductions are indicated in db for each channel separation. Each channel represents a change in frequency of $\Delta f = 1.8$ MHz. In general, the various signal levels indicated in Figure 24 will be further reduced by appropriate amounts, dependent on the actual distance separations between any transmitter and all receivers within the tropo network. In Figure 25,

Δf →

FIGURE 24
OFF-SITE
Frequency Response

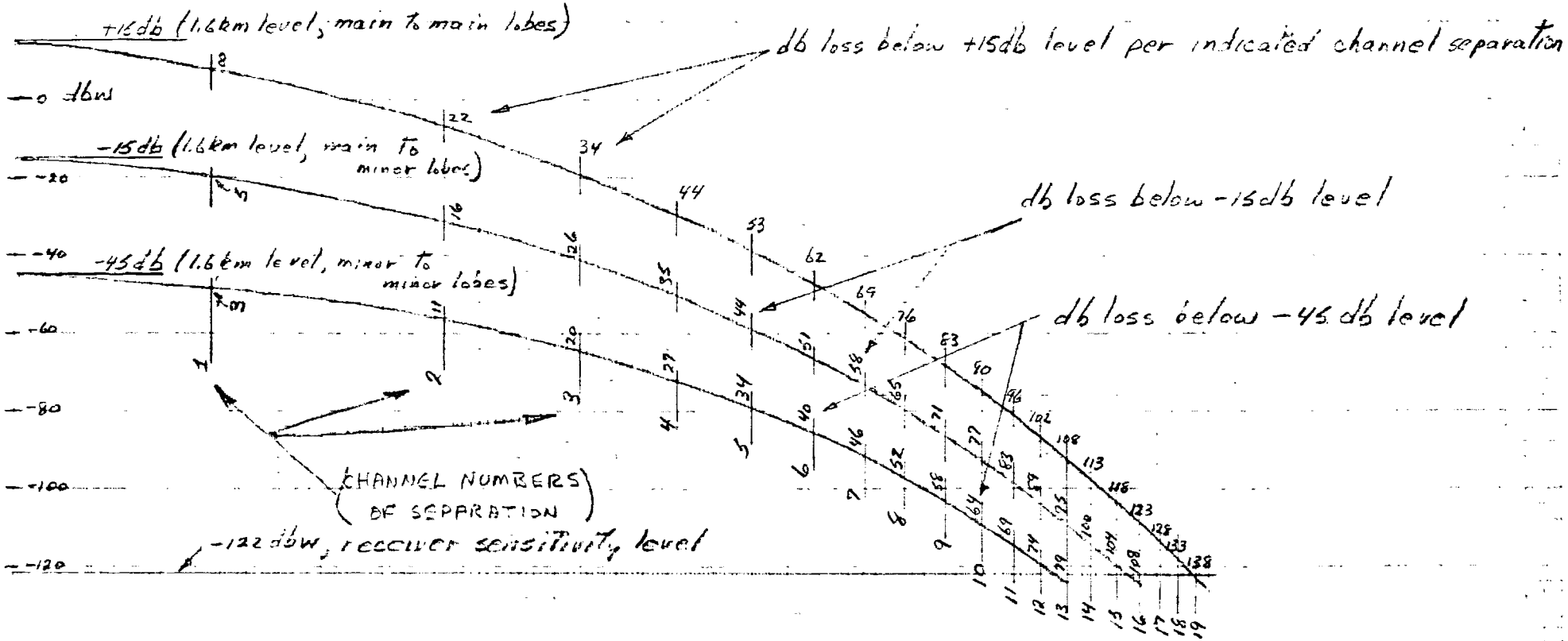

assumed maximal mean signal levels (1% values) are indicated for a temperate climate for various distances and antenna orientation circumstances. Curve 1 can be obtained by subtracting 35 db from the median (50%) values shown in the previous Figure 15 for a temperate climate, and by adding 11 db (Figure 11) for the frequency correction from 900 MHz to 4.4 GHz, which is the operating frequency of AN/TRC-90B equipment. The 35 db (mentioned above) represents several assumptions as to mean signal levels. For a temperate climate, a mean 15 db decrease in attenuation is assumed for the climatic change (winter to summer) and a 20 db decrease in attenuation is assumed for the change from 50% values to the 1% values (See previous Figure 10). All curves in Figure 25 relate to a receiver frequency which is identical to a given transmitter frequency. Curve 1 is representative of the maximal predicted signal levels for the various ranges for "major-to-major" lobe orientations. Curves 2 and 3 correspond, respectively, to "major-to-minor" and "minor-to-minor" lobe orientations. The situation represented by Curve 1 is most unlikely to occur in a network configuration, since antenna beam widths for tropo equipments are usually less than 2°. Curve 2 is also representative of an infrequent occurrence for the same reason. Curve 3 is representative of the general situation for transmitters and remote receivers in a tropo network.

8. A geographical frequency separation pattern can be constructed in the following manner. For instance, consider a transmitter operating at 4.4 GHz on one tropo link and a receiver operating on another link at a distance of 325km. If the respective antennas have a minor-to-minor lobe orientation, Curve 3 Figure 25, indicates a predicted maximum received signal level of -119dbw or 3db above receiver sensitivity, if the receiver

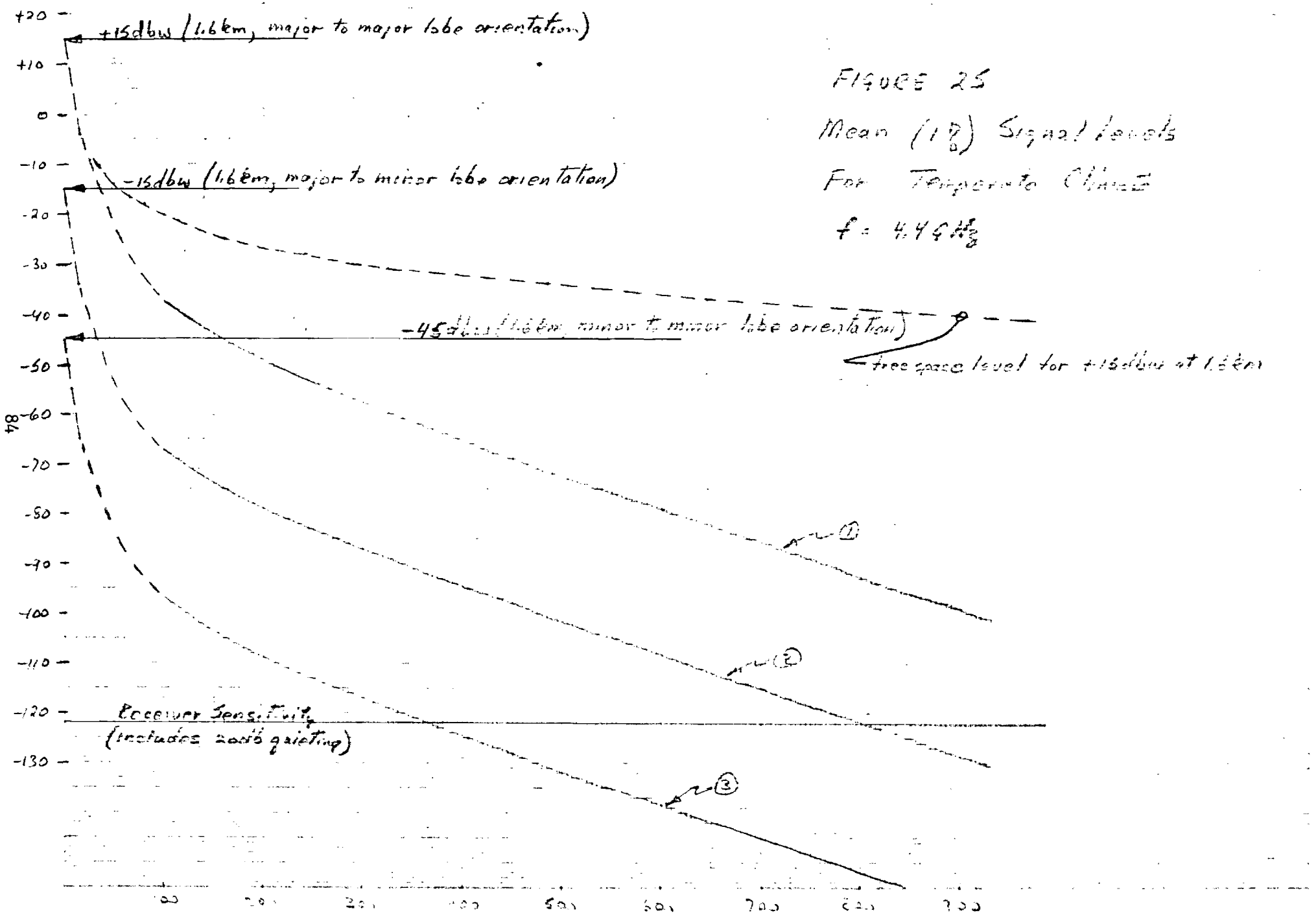

FIGURE 25

Mean (I_0) Signal Levels

For Tangent to Climb

f = 4.4 GHz

is operating on the same frequency of 4.4 GHz. Reference to Figure 24, Curve 3, indicates that a 1.8 MHz shift will provide an additional 3 db attenuation. Therefore, a one channel shift (=1.8 MHz) will provide adequate attenuation. This means that this particular receiver can be operated satisfactorily at 4400 ± 1.8 MHz, with respect to off-site interference from the given transmitter.

a. Required off-site frequency separations can also be handled in another way which is more practical with respect to manual or computer generated frequency assignments in a tropo network. Let it be assumed that the total geographical area containing a tropo network is subdivided into 25km grid squares as shown in Figure 26. If a transmitter is assumed to be located anywhere within the central grid square, then a separation distance of 325km would place the receiver approximately in any one of the 14th adjacent grid squares, for instance, as shown in grid square 17, 1 in Figure 26. As already determined above, a one channel separation is adequate for this distance, in order to prevent off-site interference between this particular receiver and a transmitter located anywhere within the central grid square.

b. In Figure 27, the required channel equations for all squares of the pattern have been indicated. These have been obtained in an identical manner to that described above, by utilization of Curve 3 in Figures 24 and 25, except for the squares along the propagation direction.

c. For the squares along the propagation direction, the following procedures have been used. A 2° antenna beam width will be contained within a 25km width for approximately 714km. If allowance is made for beam widening due to the scatter phenomena, a 50km width would be more appropriate

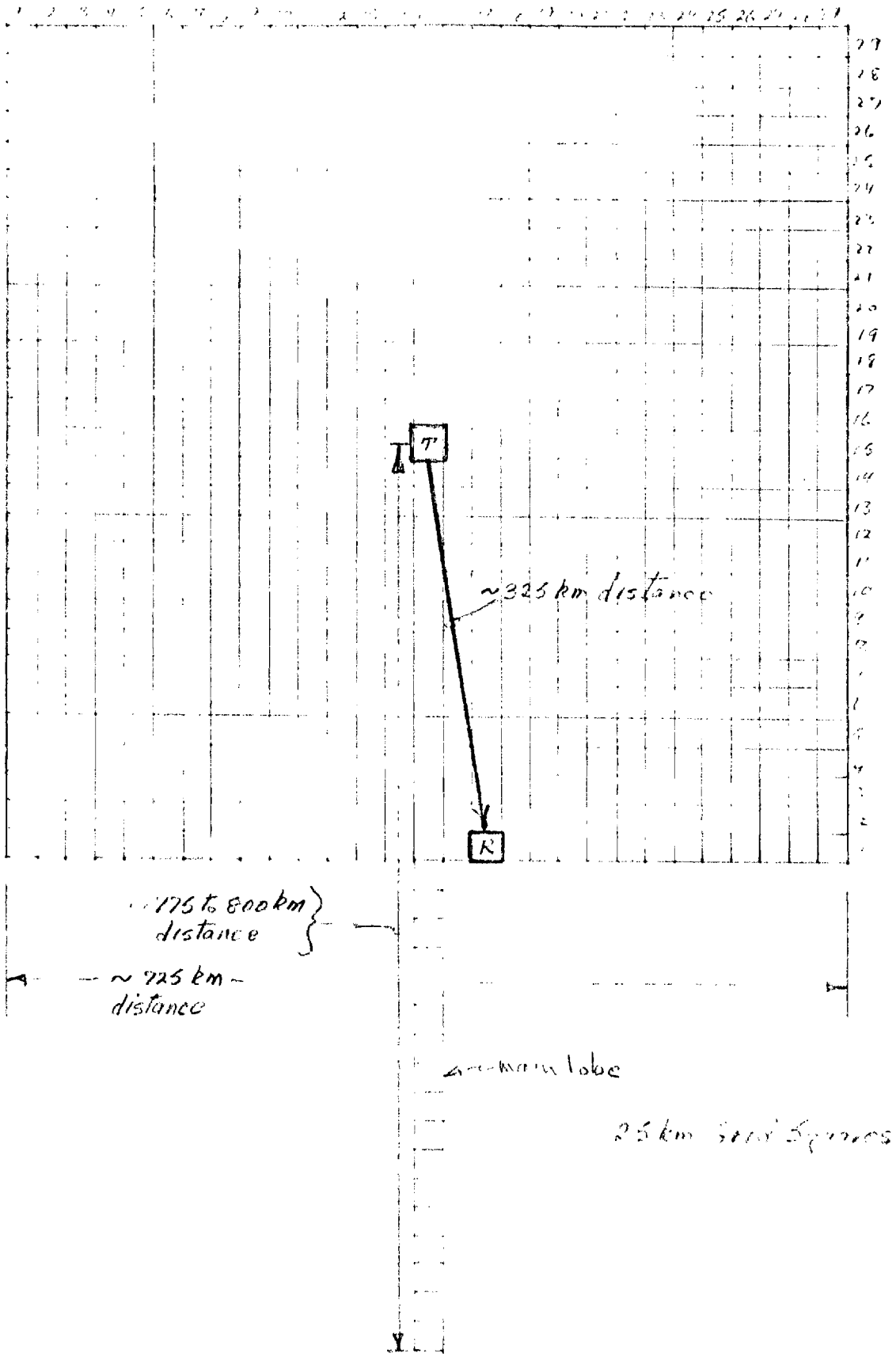

FIGURE 26

POSSIBLE SHAPE FOR

GEOGRAPHICAL FREQUENCY SEPARATION PATTERN

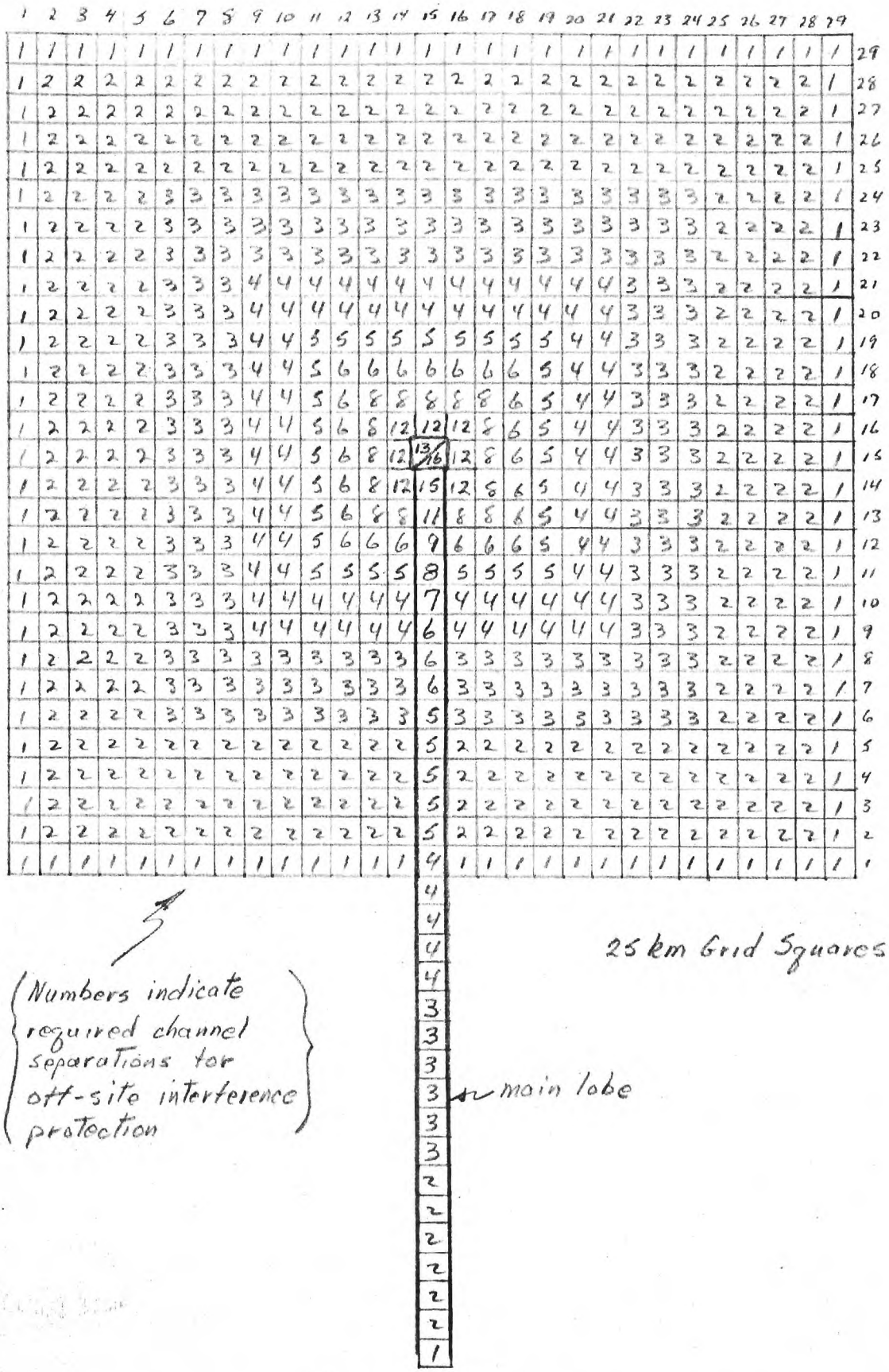

FIGURE 27
GEOGRAPHICAL FREQUENCY SEPARATION PATTERN

for the 714km distance, assuming a 4° scattered beam width. For the moment, if a 25km grid square size is maintained, the pattern is extended to 750km , as indicated in Figure 27. Furthermore, it is assumed that any remote receiver located within the 25km wide corridor from the transmitter will have its minor lobe oriented toward the transmitter. Therefore, the required channel separations can be obtained by utilization of Curve 2 in Figures 24 and 25.

9. For frequency assignments in a tropo network, the geographical locations of each terminal and link are first plotted on a map which has been subdivided into 25km grid squares. (Specific frequency assignment procedures are outlined in the following section). When any given transmitter is to be assigned an operating frequency by manual means, the geographical frequency separation pattern may be positioned on the network map such that the central grid square of the pattern overlays the map grid square containing the particular transmitter. The pattern can then be oriented (rotated on the network map) in the direction of the particular link. In general, one or more receivers will be located (on the network map) within the superposed geographical frequency separation pattern. If any of these receivers has been previously assigned to operating frequencies, then the particular transmitter (to be assigned) must be given an operating frequency which differs by the required channel separations indicated on the overlay for each previously assigned receiver. Receiver assignments may be made in a reciprocal manner.

10. The pattern shown in Figure 27 is rather large and comprises 858 discrete grid squares of 25km size. This number of grid squares will be

cumbersome in subsequent applications (either manual or computer controlled). Therefore, it is desirable to reduce the number of grid squares contained in the pattern to some minimal number. However, as the number is reduced, some degree of efficiency may be "lost" with respect to ultimate frequency assignments. This can result because of the following reasons. The use of larger grid squares obviously covers a larger discrete area for each grid square. However, off-site interference protection must be maintained for any receiver located anywhere within a grid square. When the grid square size is quite large, the change in required channel separations across the grid square may also become large. For a receiver located at one edge of the square, closest to the transmitter, adequate channel separation must be provided. However, for a receiver located at the opposite edge of the square, furthest from the transmitter, a significantly smaller channel separation may be required. Since the larger channel separation must be specified for the grid square (in order to "protect" the closest receiver) some flexibility (and perhaps efficiency) may be forfeited for possible frequency assignment to the farthest receiver within the same grid square of the pattern. The determination of an optimum size grid square for tropo networks has not yet been accomplished. The most expedient procedure is to develop an operating computer program for frequency assignments. Then the "efficiency" of frequency assignment may be examined based on the required frequencies (number of frequencies used and their spectrum) for several different sizes of grid squares and for several different networks.

11. For the purpose of this report a 50km grid square is recommended as an initial effort. Further work will be necessary to validate this choice.

An example of the geographical frequency separation pattern for 50km grid squares is shown in Figure 28. This pattern is small and can be handled relatively easily by manual or computer means.

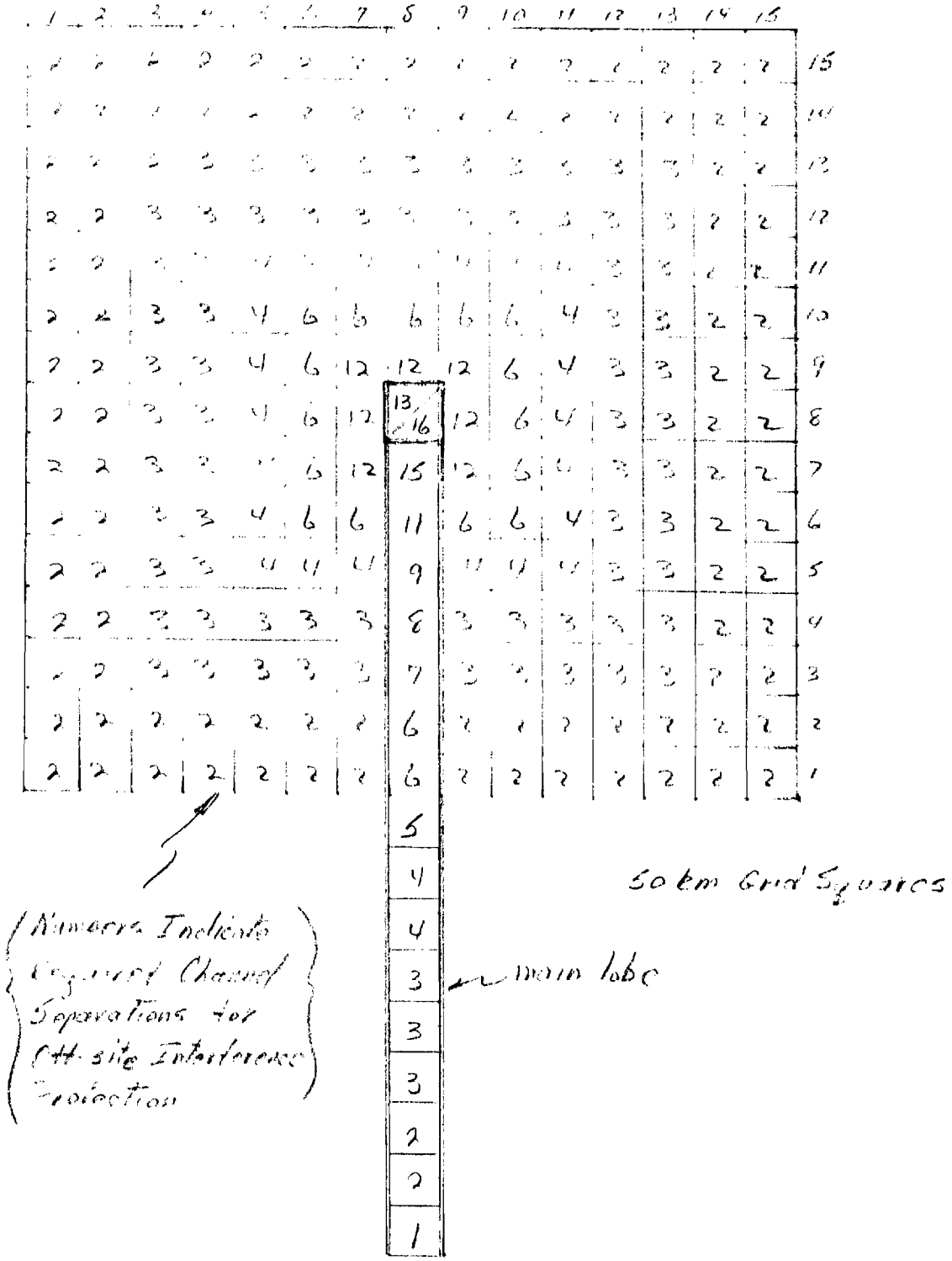

FIGURE 28

SUGGESTED

GEOGRAPHIC FREQUENCY SEPARATION PATTERN

G. Recommended Frequency Assignment Procedures

1. Within the scope of this report there has not been sufficient time to develop an operational computer program for frequency assignments in tropo networks. Therefore, the recommended procedures are presented only in outline form. More detailed discussions on operating procedures can be inferred from a study of reference 38.

2. For practical computer applications, the number of input parameters for any tropo-network problem should be maintained at a minimal number. On the other hand, the prediction of received signal levels for any given tropo link is rather complex. Current procedures, at best, yield predictions which may be in error by 10 db or more for any given application. As mentioned in the previous sections, the mean "worst case" conditions have been assumed, and some possible corrections thereto have been recommended for specific cases. A sophisticated computer program for the solution of tropo network problems may be subdivided into two parts: a program for computing predicted received signal levels for any given tropo link, and a program for automatic frequency assignment of each link within a tropo network. The two parts may be separate and distinct functions since the procedures to be utilized are not interrelated.

3. For computation of received signal levels, the following control parameters might be utilized as inputs:

a. Transmitter power level.

b. Receiver sensitivity level.

c. Path distance, or transmitter and receiver locations.

d. Climatic region.

e. Mean values of refractive index and/or gradient, if available.

f. Expected signal variations and fluctuations (σ), if available from previously obtained data on other operating links within the area.

g. Operating frequency band.

h. Transmitter and receiver antenna elevation angles.

i. Antenna gains.

j. Antenna beam width.

k. Diversity configurations, if applicable.

l. Spherical diffraction path data, if applicable and if desired. Additional input data would include transmitter and receiver elevations, elevations of the terminal horizons, as well as the highest elevation between terminal horizons.

4. For computation of received signal levels, the computer program would maintain storage for the following items.

a. Empirical curves (perhaps tables) for the various climatic regions.

b. Tables related to expected signal variations and fluctuations. If separate parameter inputs are desired for these items, such inputs would preempt the stored table usage.

c. Subroutine for generating expected diffraction signal levels, based on optional input data. If no data are input, these procedures would be omitted in the computational processes.

d. Computer output could be adjusted to produce transmitter and receiver locations together with the predicted mean signal levels and variations for each link. If transmitter and receiver locations are input instead of path distance (item c in paragraph 3 above), these data may be utilized subsequently for the frequency management program.

5. For the assignment and management of frequencies in a tropo link, the computer program might utilize the following inputs.

a. Numbers for each transmitter and associated receiver for a given link. This can best be accomplished by the consecutive numbering of each separate site in the tropo network. Then each link can be specified by the related site numbers. (It is possible for this step to be accomplished by computer programming, such that each input link, involving a particular transmitter and receiver location, can be related to appropriate site numbers which are machine assigned. See following item b.)

b. The location of each transmitter and associated receiver for each link. These data could be obtained and input directly, for instance, from a military map of the network area, providing that a resident subroutine program could compute the corresponding locations, based on the grid square size to be utilized. Otherwise, these data on terminal locations would have to be converted to the appropriate grid square locations, before being input to the computer. In addition, if it is desired that network site numbers be machine generated, instead of being preassigned and input to the computer, a subroutine must be provided for this purpose. For instance, as each transmitter and associated receiver location were input for each link, the subroutine program would assign sequential site numbers to the terminals, after checking to verify that the terminal to be assigned a new site number is not colocated with a previously assigned site number. If this situation occurs, the terminal to be assigned would be given the same site number as previously designated for the colocated terminal.

c. The number of links operating out of a given site. (If the subroutines mentioned in a and b above were available, these data could be generated automatically by the subroutine procedures.)

d. The particular frequencies (or assignable channels) which have been allocated to network usage.

e. The frequency separation requirements for the particular network equipment in use. These include T-R(SS), T-R(DS), T-T(DS), and R-R(DS), as well as any forbidden frequency separations. Finally, the applicable geographical frequency separation pattern must be input, relating to off-site frequency separations.

f. A particular frequency blocking plan[38] must be selected. (This selection includes several options which relate to the network size, number of links, link arrangement, etc. Dependent on network circumstances, there may exist one of several different frequency blocking plans which could be utilized. For instance, for any given link, a transmitter can be assigned on one frequency, and its associated receiver (involved in the return link) can be immediately assigned on another frequency which must differ by 110 MHz, for AN/TRC-90B equipment. Therefore, a so-called two-block frequency plan might be utilized whereby the allotted frequencies (or channels) are divided into two separate groups. For instance, one group of frequencies can be used for a particular transmitter assignment on a given link, and the other group of frequencies can be utilized for the associated receiver assignment on the same given link.)

6. For frequency assignment, the following general procedures may be used. (See reference 38 for more detailed discussions.)

a. A connectivity matrix is machine constructed, which relates all sites to their corresponding connected (or linked) sites. In general, this procedure orders the sites (and corresponding links) according to decreasing numbers of connections at a given site. This procedure is

preparatory to frequency assignment and ultimately enables a more efficient usage of the available frequencies. There is also an optional input related to priority links. Thus, if a given link(s) has high priority, this link(s) can be automatically placed at the start of the connectivity matrix site listing.

b. Dependent on the pre-selected frequency plan (item f in paragraph 5 above), the computer program can then initiate appropriate frequency assignment to each transmitter, taken in sequence from the connectivity matrix site listing. Subsequently, appropriate frequency assignments can be made to each associated receiver, taken in sequence. It is also possible to assign frequencies (in pairs) to each link, taken in sequence. However, significant improvements in frequency usage were obtained for radio relay networks[38] utilizing the former frequency assignment procedure (first, transmitter assignments in sequence, and, second, associated receiver assignments in sequence).

7. The computer program for radio relay networks[38] also permits post-environmental additions and deletions of links. The procedures utilized do not require any frequency changes for previously assigned links. In addition, the assignments of frequencies to the new post-environmental additions maintain efficient usage of the available frequencies. The same type of accomplishments should be available for tropo networks.

8. Several options are available for computer outputs from radio relay networks problems. These same options, if desired, should be available for tropo networks.

9. Further effort will be necessary in order to construct the appropriate computer programs for use in tropo networks. In addition, further study would be desirable on the empirical relationships presented in Section D. A satisfactory use of these relationships needs to be established by means of data comparisons with a large number of operating tropo links. On the other hand, any changes in these proposed relationships would not affect any developed computer program. Such changes would only necessitate elemental changes in the stored data of computer tables.

H. References

1. International Geodesic and Geophysical Union, 12th General Assembly, Helsinki, July-August, 1960.

2. Recommendation 369, Comite' Consultatif International des Radio Communications, 10th Plenary Assembly, Geneva, 1963.

3. Vergara, W., J. Levatich, and T. J. Carroll, "VHF Air-Ground Propagation Far Beyond the Horizon and Tropospheric Stability," Trans. IRE, AP 10, 1962.

4. Chambers, J., "Successful UHF Communications for 2540 Miles at 144 and 222 MHz," paper presentation, IRE-URSI, Joint Fall Meeting, Washington, D. C., October 20, 1959.

5. Chisholm, J. H., "Recherches Experimentales sur la Diffusion Angulaire et sur les Possibilities d'Utilisation de la Propagation Tropospherique," Onde Electr, 37, 1957.

6. Waterman, A. T., "A Rapid Beam Swinging Experiment in Transhorizon Propagation," Trans. IRE, AP 6, 1958.

7. Crawford, A. B., D. C. Hogg, and W. H., Kummer, "Studies in Tropospheric Propogation Beyond the Horizon," Bell Sys. Tech. J., 38, 1959.

8. Misme, P., "Interpretations des Mesures Meterologiques," Ann. Telec., 13, 1958.

9. DuCastel, F., Tropospheric Radio Wave Propagation Beyond the Horizon, New York: Pergamon Press, 1966, 21.

10. Gordon, W. E., "Radio Scattering in the Troposphere," Proc IRE, 43, 1955.

11. Villars, V., and V. F. Weisskopf, "On the Scattering of Radio Waves by Turbulent Fluctuations of the Atmosphere," Proc IRE, 43, 1955.

12. Silverman, R. A., "Turbulent Mixing Theory Applied to Radio Scattering," J. Appl. Phys., 27, 1956.

13. Wheelan, A. D., "Spectrum of Turbulent Fluctuations Produced by Convective Mixing of Gradients," Phys Rev, 105, 1957.

14. Megaw, E. C. S., "The Scattering of Electromagnetic Waves by Atmospheric Turbulence," Nature, London, 166, 1950.

15. Koono, T., M. Hirai, R. Inone, and Y. Ishizawa, "Antenna Beam Reflection Loss and Signal Amplitude Correlation in Angle Diversity Reception in UHF Beyond Horizon Communications," J Rad Res Lab, Japan 9, 1962.

16. Tremblay, R., "Etude Theorique et Experimentale des Problemes de Fluctuations Rapides en Propagation Tropospherique," Ann. Radio, 17, 1962.

17. Carroll, T. J., "Internal Reflection in the Troposphere and Propagation Beyond the Horizon," Trans IRE, AP 9, 1952.

18. Carroll, T. J., and R. M. Ring, "Propagation of Short Radio Waves in a Normally Stratified Troposphere," Proc IRE, 43, 1955.

19. Norton, K. A., P. L. Rice, and L. E. Vogler, "The Use of Angular Distance in Estimating Transmission Loss and Fading Range for Propagation through a Turbulent Atmosphere over Irregular Terrain," Proc IRE, 43, 1955.

20. Svien, A. S. and J. C. Dominque, "Tropospheric Scatter Propagation Characteristics," Nat Conv Rec IRE, Part 1, 1959.

21. Chisholm, J. H., P. A. Portman, J. T. de Bettencourt, and J. F. Roche, "Investigation of Angular Scattering and Multipath Properties of Tropospheric Propagation of Short Radio Waves Beyond the Horizon, Proc IRE, 43, 1955, and related document, S. A. D. T. C., "Ace High," R 1, 1957.

22. "Study and Investigation of Tropospheric Scattering," RCA Report, 1956.

23. Felsenheld, R. A., H. Haustad, J. L. Jatlow, D. J. Levine, and L. Pollack, "Wideband UHF Over the Horizon Equipment," Elect Comm, 4, 1959.

24. Parry, C. A., "A Formalized Procedure for the Prediction and Analysis of Multichannel Tropospheric Scatter Circuits," Trans IRE, CS 7, 1959.

25. Bean, B. R., and F. M. Meaney, "Some Applications of the Monthly Median Refractivity Gradient in Tropospheric Propagation," Proc IRE, 43, 1955.

26. Bean, B. R., and J. D. Horn, "The Radio Refractive Index Climate Near the Ground," J. Res. Nat. Bur. Std., 63D, 1959.

27. Bean, B. R., L. Fehlharber, and J. A. Grosskopf, "A Comparative Study of the Correlation of Seasonal and Diurnal Cycles of Transhorizon Radio Transmission Loss and Surface Refractivity," J. Res. Nat. Bur. Std., 66D, 1962.

28. Bean, B. R., and B. Thayer, "Comparison of Observed Atmospheric Radio Refraction Effects with Value Predicted through the Use of Surface Weather Observations," J. Res. Nat. Bur. Std., 67D, 1963.

29. Report 233, Comité Consultatif International des Radio Communications, 1963.

30. Bean, B. R., "Some Meteorological Effects on Scattered Radio Waves, IRE Trans, CS 4, No. 1, 1956.

31. Recommendation 132, Comité Consultatif International des Radio Communications, Los Angeles, 1959.

32. Document 64, Comité Consultatif International des Radio Communications, Cannes, 1961.

33. Booker, H. G., and J. J. de Bettencourt, "Theory of Radio Transmission by Tropospheric Scattering Using Very Narrow Beams," Proc IRE, 43, 1955.

34. Staras, H., "Antenna to Medium Coupling Loss," Trans. IRE, AP, 1957.

35. Engelbrecht, L., "Tactical Tropospheric Scatter Techniques," Eng. Bulletin, Vol. 16, No. 2, Military Electronics Division, Motorola, Inc., 1968.

36. Chisholm, J. H., "Progress of Tropospheric Propagation Research Related to Communication Beyond the Horizon," Trans IRE, CS 6, 1956.

37. Boithias, L., an F. DuCastel, "Etude d'un Faisceau Hertzien Transhorizon en Afrique Occidentale," Onde Elect, 11, 1960.

38. Hungerford, E. T., O. B. Francis, K. E. Hoenes, F. R. Pinkerton, L. J. Gallaher, J. P. McGovern, and I. E. Perlin, Development of a Frequency Assignment System for Radio Relay Networks, Vols I-IV, Rich Electronic Computer Center, Georgia Institute of Technology, Contract DA 28-043-AMC-01551(E), for Electromagnetics Directorate, Office of the Assistant Chief of Staff, Communications-Electronics, Department of the Army, 1969.